1998-12

Biomechanical response of the human body inside a military vehicle exposed to mine explosion

Lee, KyuSang

Monterey, California. Naval Postgraduate School

NAVAL POSTGRADUATE SCHOOL
MONTEREY, CALIFORNIA

THESIS

BIOMECHANICAL RESPONSE OF THE HUMAN BODY INSIDE A MILITARY VEHICLE EXPOSED TO MINE EXPLOSION

by

KyuSang Lee

December 1998

Thesis Advisor: Young W Kwon

Approved for public release; distribution is unlimited.

REPORT DOCUMENTATION PAGE

Form Approved OMB No. 0704-0188

1. AGENCY USE ONLY *(Leave blank)*	2. REPORT DATE	3. REPORT TYPE AND DATES COVERED
	December 1998.	Master's Thesis

4. TITLE AND SUBTITLE:
BIOMECHANICAL RESPONSE OF THE HUMAN BODY INSIDE A MILITARY VEHICLE EXPOSED TO MINE EXPLOSION

5. FUNDING NUMBERS

6. AUTHOR(S)
KyuSang, Lee

7. PERFORMING ORGANIZATION NAME(S) AND ADDRESS(ES)
Naval Postgraduate School
Monterey CA 93943-5000

8. PERFORMING ORGANIZATION REPORT NUMBER

9. SPONSORING/MONITORING AGENCY NAME(S) AND ADDRESS(ES)

10. SPONSORING/MONITORING AGENCY REPORT NUMBER

11. SUPPLEMENTARY NOTES
The views expressed here are those of the authors and do not reflect the official policy or position of the Department of Defense or the U.S. Government.

12a. DISTRIBUTION/AVAILABILITY STATEMENT
Approved for public release; distribution is unlimited.

12b. DISTRIBUTION CODE

13. ABSTRACT *(maximum 200 words)* Biomechanical response of the human body inside a military vehicle exposed to AP mine explosion was studied using the finite element method. The main focus was placed on evaluation of the injury potential of the human body, particularly the brain, neck (cervical spine), and legs. Injury criteria used to evaluate the injury potential were HIC, IARV's, and some others. The military vehicle used in this research was M1097A2, the basic model of HUMVEE. In addition to the evaluation of the injury potential, some design modifications to the present vehicle were considered in order to reduce the injury potential to the crew of the vehicle.

14. SUBJECT TERMS
Optimization of Nonlinear isolation

15. NUMBER OF PAGES
68

16. PRICE CODE

17. SECURITY CLASSIFICATION OF REPORT	18. SECURITY CLASSIFICATION OF THIS PAGE	19. SECURITY CLASSIFICATION OF ABSTRACT	20. LIMITATION OF ABSTRACT
Unclassified	Unclassified	Unclassified	UL

NSN 7540-01-280-5500

Standard Form 298 (Rev. 2-89)
Prescribed by ANSI Std. 239-18 298-102

Approved for public release; distribution is unlimited

BIOMECHANICAL RESPONSE OF THE HUMAN BODY INSIDE A MILITARY VEHICLE EXPOSED TO MINE EXPLOSION

KyuSang Lee
Captain, Korean Army
B.S.M.E., Korean Military Academy, 1989

Submitted in partial fulfillment of the
Requirements for the degree of

MASTER OF SCIENCE IN MECHANICAL ENGINEERING

from the

NAVAL POSTGRADUATE SCHOOL
December 1998

Author: [redacted]
KyuSang Lee

Approved by: [redacted]
Young W. Kwon

[redacted]
Terry R. McNelly, Chairman
Department of Mechanical Engineering

ABSTRACT

Biomechanical response of the human body inside a military vehicle exposed to AP mine explosion was studied using the finite element method. The main focus was placed on evaluation of the injury potential of the human body, particularly the brain, neck (cervical spine), and legs. Injury criteria used to evaluate the injury potential were HIC, IARV's, and some others. The military vehicle used in this research was M1097A2, the basic model of HUMVEE. In addition to the evaluation of the injury potential, some design modifications to the present vehicle were considered in order to reduce the injury potential to the crew of the vehicle.

TABLE OF CONTENTS

ACKNOWLEDGMENTS

I would like to express my great appreciation to Professor Young W. Kwon for his support throughout this research. His dedicated guidance has significantly enhanced my education at the Naval Postgraduate School.

I also extend my gratitude to Professor Young S. Shin for allowing me to use his excellent laboratory facilities. I would also like thank Dr. Park for sharing his valuable experience, LT. Linda E. Craugh, USN and Pamela L. Silva at the Naval Postgraduate School for helping me to overcome my language barrier in English, and most important, my wife Miok and daughter, Hakyong, for their patience and understanding.

I. INTRODUCTION

The wide range use of landmines by both prominent and third world countries has made their use and control a critical world wide issue. Approximately 74 countries are using landmines for military operation or exposed to unexpected mine explosion damages. Therefore, military operations are evolving with respect to control of landmine and protecting human beings from the effects of mine explosion. This situation has triggered many civilian research centers and defense agencies to expend vast efforts to sweep mines and develop protection equipment.

This research is a part of these efforts and, the objective is to model and simulate the biomechanical response of military personnel inside a military vehicle exposed to a mine explosion using the finite element method. Focus is placed on evaluation of injury potential of military personnel, in particular brain damage, neck (cervical spine) injury, and leg injury. Furthermore, simple modifications of the military vehicle are considered in order to reduce injury potential of the human body.

The military vehicle used for this research is the M1097A2, normally called HUMVEE, which is widely used in military operations. The landmine selected for this study as the source of the explosive load is PMN, an anti-personnel mine. The PMN is widely used in many Communist and third world countries. This study models the human body as a skeleton structure consisting of the head, spine, pelvis, and legs.

II. BACKGROUND

A. ANATOMY OF HUMAN BODY

This chapter describes the general human skeleton including its material properties, connectivity, and movements. However, ribs, scapulars and arms are excluded for research purposes. Figure 1 shows the human skeleton and its anatomy.

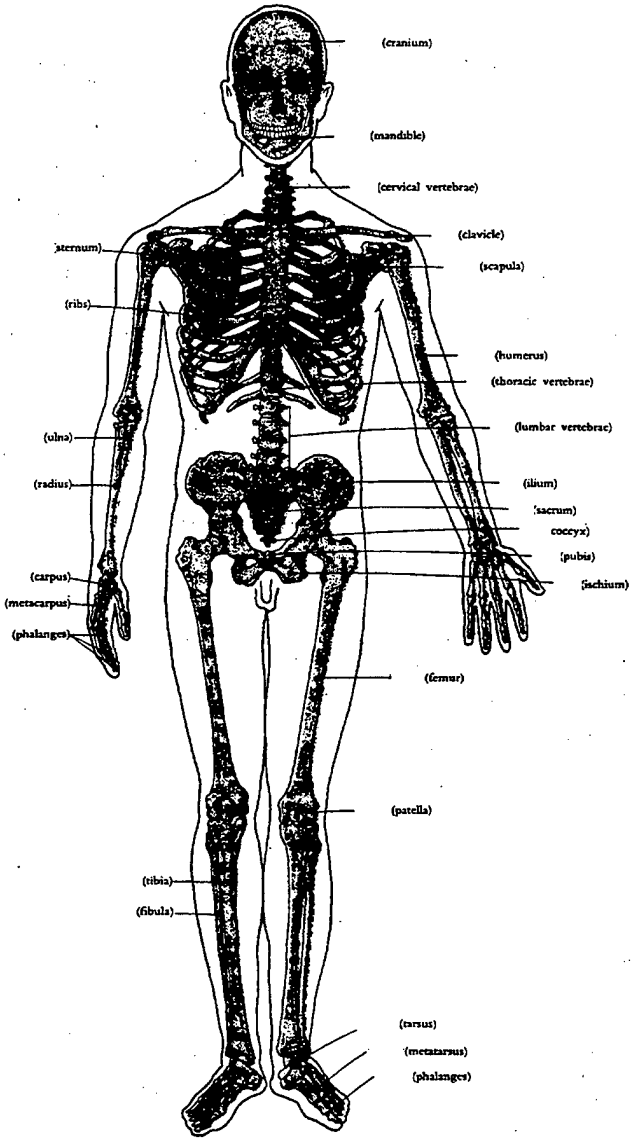

Figure 1. Human Skeleton (Anterior View) [Ref. 1]

1. Head

The head consists of the scalp, skull, meninges, nervous system, and brains. The scalp encircles the skull with its muscular layer, the skull is the bony part of a head with thickness between 4 to 7 mm, and meninges between brain and skull support and protect the brain. The focus of the head injury is given to the brain damage caused by external acceleration in this research. The fracture of the skull and head's detail deformation is not considered. In order to estimate the acceleration effect over the brain, the weight and the center of mass of the head are important. Earlier research on the human body showed that the head of a 77kg male weighs 6.18 kg [Ref. 2].

2. Spine

The spine consists of 24 vertebrae, 23 discs and surrounding ligaments. It is divided vertically into three major sections; cervical, thoracic, and lumbar spines as shown in Figure 2. The upper seven vertebrae are called the cervical spine, known as neck, and give connection between the head and the trunk. In order to describe the unique location of each vertebra, a naming convention is used. The initial of each spinal name is combined with a number. That is, the uppermost cervical vertebra is called 'C1' and C2 is located right below C1. Figure 3 shows how two vertebrae are connected to each other. Each vertebra varies in dimensions depending on age, sex, and ethnic group. Table 1 shows the dimensions of the vertebrae. Another consideration is given to ligaments. Ligaments are uniaxial structures surrounding the vertebrae and they act like rubber bands. They then give resistance under tension but buckle when subjected to compression. The main function of ligaments is to allow proper spinal motion, without damaging the spinal cord and structure, and to support the vertebrae and trunk with muscle. Figure 4 shows how they are attached to the vertebrae. The geometric properties of ligaments are given in Table 2.

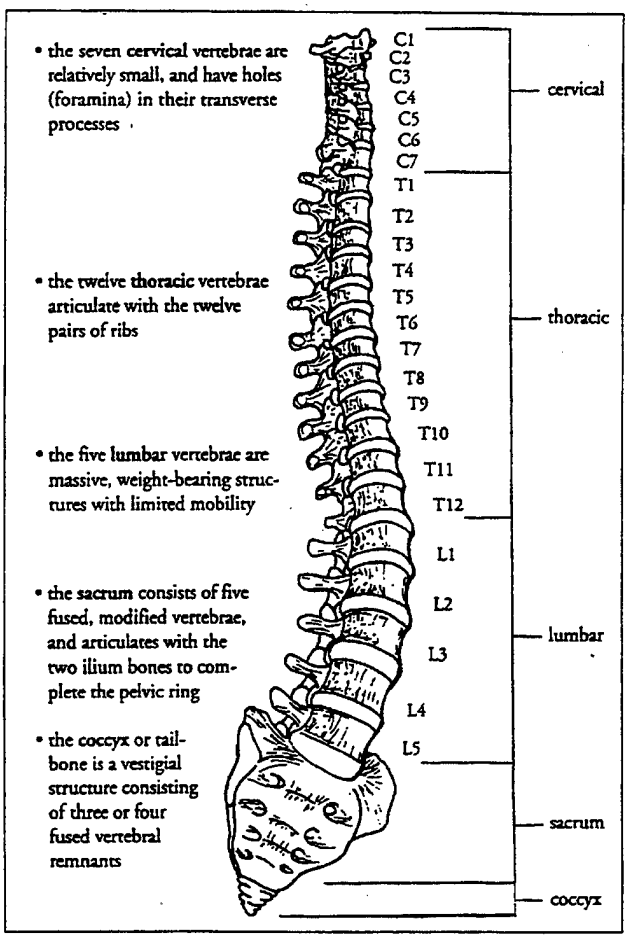

Figure 2. Spinal Column [Ref. 3]

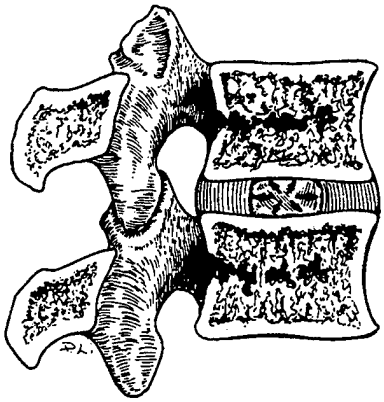

Figure 3. Connectivity of Two Vertebrae [Ref. 4]

Table 1. Pedicle Dimensions at Selected Cervical, Thoracic, and Lumber Levels [Ref. 4]

	Width (mm)	Height (mm)	Angle With Sagittal Plane (degrees)	Angle With Transverse Plane (degrees)
C3	6 (4–8)	8 (6–10)	41 (20–55)	−6 (−16–4)
C5	6 (4–8)	7 (5–9)	39 (24–54)	0 (−10–10)
CT	7 (5–9)	8 (6–10)	30 (15–45)	6 (4–16)
T1	8 (5–10)	10 (7–15)	27 (16–34)	13 (4–25)
T5	5 (3–7)	12 (7–14)	9 (2–19)	15 (7–20)
T9	6 (4–9)	14 (11–16)	8 (0–11)	16 (9–14)
T12	7 (3–11)	16 (12–20)	−4 (−17–15)	12 (7–16)
L1	9 (5–13)	15 (11–21)	11 (7–15)	2 (−13–15)
L2	9 (4–13)	15 (10–18)	12 (5–18)	2 (−10–13)
L3	10 (5–16)	15 (8–18)	14 (8–24)	0 (−10–12)
L4	13 (9–17)	15 (9–19)	18 (6–28)	0 (−6–7)
L5	18 (9–29)	14 (10–19)	30 (19–44)	−2 (−8–6)

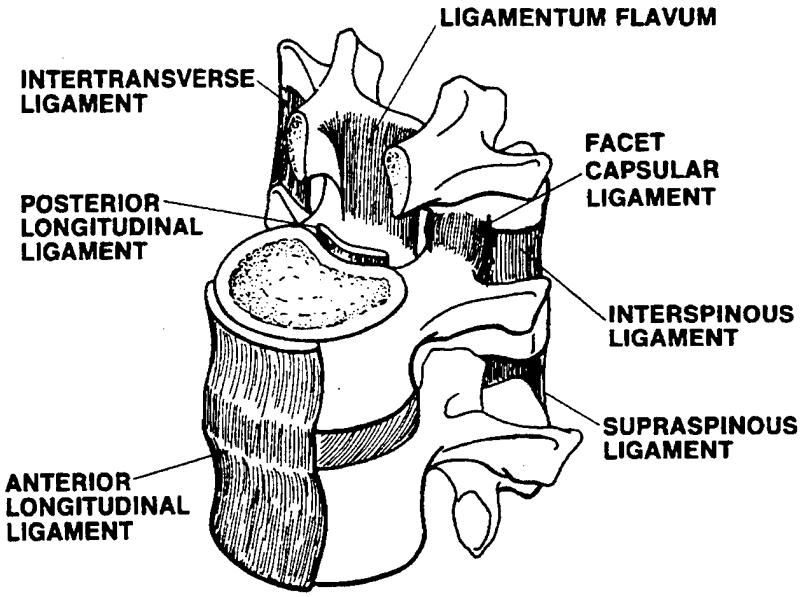

Figure 4. Ligaments of the Spine [Ref. 4]

Table 2. Cross Sectional Areas and Lengths of Spinal Ligaments [Ref. 4]

Region	Level	Ligament	Cross-sectional Area (mm^2)	Length
Cervical	C1–C2	Transverse	18	20
		Alar	22	11
Lumbar		ALL	53	13
		PLL	16	11
		LF	67	19
		CL	—	—
		ISL	26	—
		SSL	23	11

Key
ALL = anterior longitudinal ligament;
PLL = posterior longitudinal ligament;
LF = ligamentum flavum;
CL = capsular ligament;
ISL = interspinous ligament;
SSL = supraspinous ligament.

The disc is the inter-vertebral material with an anisotropic physical structure and viscoelastic property. It carries the compressive loading to the trunk along with the facet joints under the various forces and moments [Ref. 4]. Figure 5 and Table 3 show a disc from the spinal column and its stiffness. The spinal cord is clinically an important component in the spinal column. This sensitive cord is enclosed within the vertebral canal. In a mechanical perspective, however, it is not important and hence excluded in the spinal structure of this research.

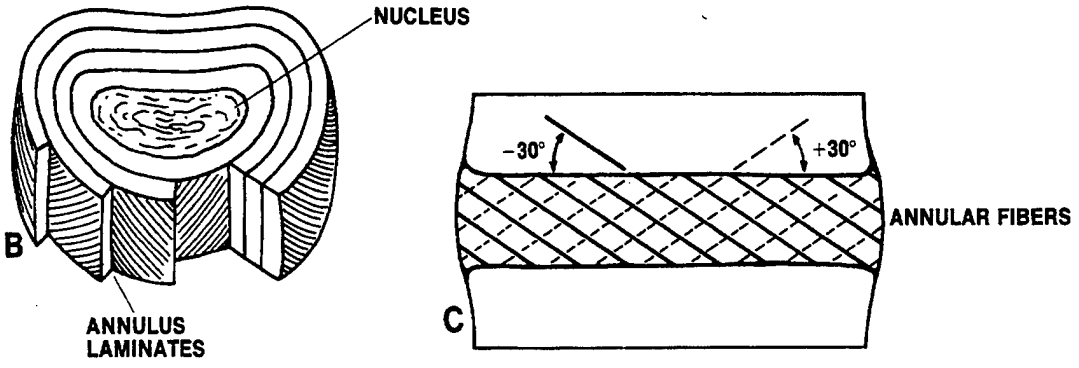

Figure 5. Intervertebral Disc [Ref. 3]

Table 3. Stiffness Coefficients of the Intervertebral Disc [Ref. 3]

Authors	Stiffness Coefficients*	Maximum Load*	Spine Region
Compression ($-Fy^{+}$)			
Virgin, 1951	2.5 MN/m	4500 N	Lumbar
Hirsch & Nachemson, 1954	0.7 MN/m	1000 N	Lumbar
Brown, et al., 1957	2.3 MN/m	5300 N	Lumbar
Markolf, 1970	1.8 MN/m	1800 N	Thoracic & lumbar
Moroney, et al., 1988	0.5 MN/m	74 N	Cervical
Tension ($+Fy^{+}$)			
Markolf, 1970	1.0 MN/m	1800 N	Thoracic & lumbar
Shear (Fx, Fz^{+})			
Markolf, 1970	0.26 MN/m	150 N	Thoracic & lumbar
Moroney, et al., 1988	0.06 MN/m	20 N	Cervical
Axial Rotation (My^{+})			
Fairfan, et al., 1970	2.0 Nm/deg	31 Nm	Lumbar
Moroney, et al., 1988	0.42 Nm/deg	1.8 Nm	Cervical

* N = newton, kN = 1000 newton, MN = 1,000,000 newton, Nm = newton meter
To convert to the inch-pound system, multiply by the following numbers:
(MN/m) × 5600 = lbf/in (Nm/deg) × 0.738 = in lbf/deg (N) × 0.225 = lbf (Nm) × 0.738 = in lbf

3. Pelvis

"Pelvis is the lower part of the trunk of the human body, bounded at the front and on either side by the hipbone, and at the back by the sacrum and coccyx, the lowest part of the spinal column" [Ref. 5]. Pelvis forms a ring shape between the spinal column and lower femurs. As defined above, it is composed of two hip bones, a sacrum, and coccyx. Pelvis is functionally the only path to transmit the weight load of the upper body and connected to femurs with socket-like joints in order to give more degrees of freedom for leg motion. Bone structure between the male and female are different because of birth canal. This study uses a very simplified model. Figure 6 shows the frontal view of the pelvis.

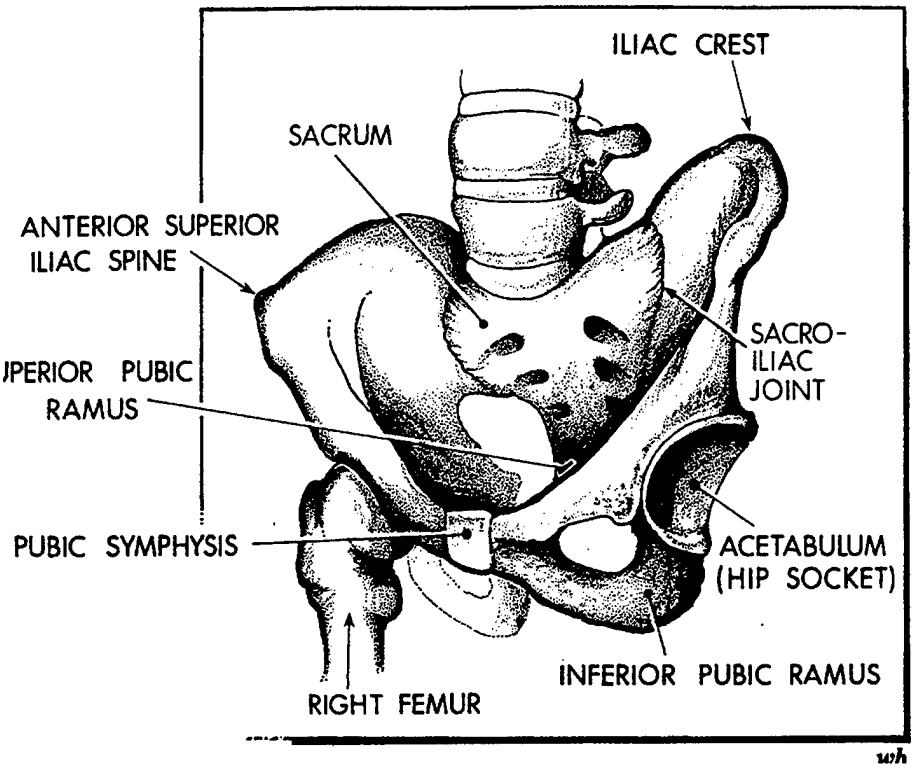

Figure 6. Pelvis [Ref. 6]

4. Lower Limbs (Legs and Feet)

The lower limbs can be divided into six major regions: the hip, thigh, knee, leg, ankle, and foot. Each part consists of bony structures, surrounding ligaments or muscles, and joints. The detail of each region is not considered in this research. However, the bony structure of the leg, thigh, foot, and joints will be modeled in the finite element analysis in the following section. The leg and thigh are composed of four bones: femur, patella, tibia and fibula. Figure 7 shows the bony structure of the lower limbs. The motion of the leg and foot depends on the joints between the acetabulum (hip socket) and femur, and between femur and tibia. The motion between the femur and tibia is restricted to primarily one rotational degree of freedom within a given limit. Figure 8 and Figure 9 show the structure of the foot and various motions at the joints of the leg.

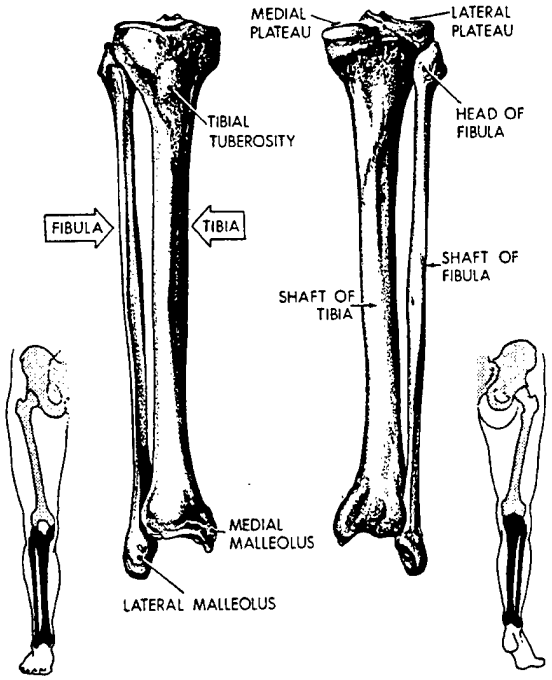

Figure 7. Bony Structure of Lower Limbs [Ref. 6]

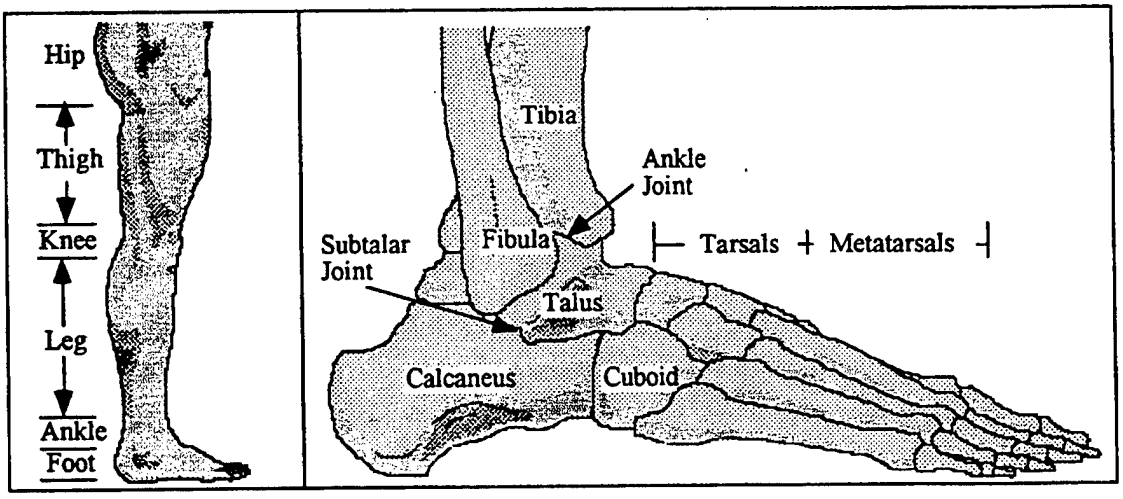

Figure 8. Anatomy of the Lower Limb and Foot [Ref. 7]

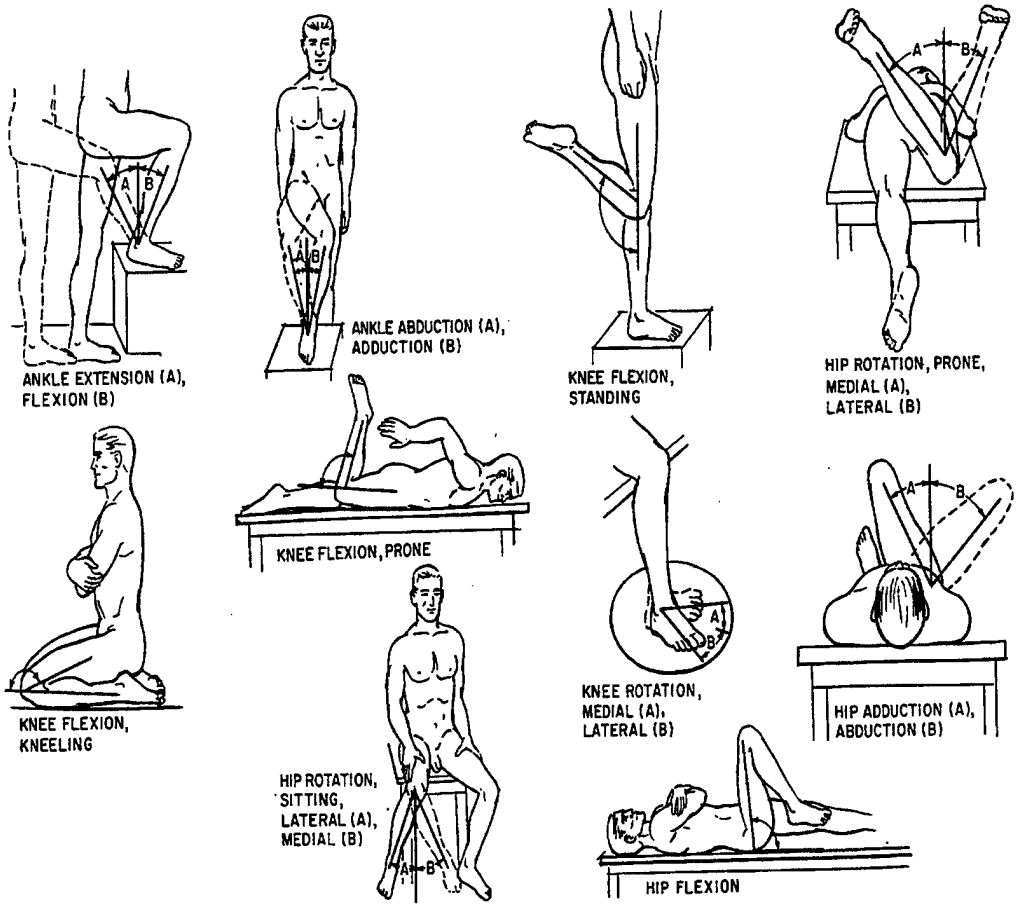

Figure 9. Motion at the Joints of the Leg and Foot [Ref. 2]

B. LITERATURE SURVEY

Reviewing literature, many similar works have been done in the area of automobile crash injuries by SAE (the Society of Automobile Engineers) and many others. Research done so far can be categorized into several subtopics depending on their interests, methodological differences they used to evaluate the injury, and accomplishments etc. This study requires background information on the biomechanics of the human body, the characteristics of the human injury, and modeling technique, such as the finite element method. The literature survey was conducted in this regard.

Goldstein, Frankenburg, and Kuhn [Ref. 8] reviewed and summarized the current perspectives on the mechanical characteristics of bone in their research. They strongly recommended that providing universal material constants to characterize the properties of bones is not possible, since the bone is an anisotropic, nonlinear, and viscoelastic material and has variety in its structure as a function of mechanical or physiologic demand. Their research also summarized studies from several investigators for the mechanical and architectural properties of bones. For additional information concerning details of bone properties, refer to [Ref. 8].

For brain injury, Melvin, Lighthall, and Ueno [Ref. 9] gave a good introduction. They classified experimental models of the brain injury into three sub-types: head-impact model, head acceleration model, and direct brain deformation model compared to two clinical brain injury categories: diffuse injury and focal injury [Ref. 9]. They also summarized many previous studies related to brain injury and injury criteria. Details are given in [Ref. 9].

The research of McElhaney and Myers [Ref. 10] provides a brief anatomy and structure of the human neck. They classified the mechanism of cervical spine injuries and summarized the properties and tolerance of the cervical spine. Table 4 shows the classifications of cervical spine injuries.

Robert Levine [Ref.11] studied injuries to the extremities: upper and lower. These are classified into four types: bone fracture, dislocation, ligament injury, and nerve injury. Fractures were subcategorized using several descriptive terms: displaced and

undisplaced fracture, impacted and angulated fracture, or comminuted and non-comminuted fractures, etc. For further detail, see [Ref. 11].

The finite element method is a very popular technique for modeling the complex human body. There have been intensive studies on how to model the human body. Most of them modeled specific details of small such as femurs, tibias, heads, respectively. On the other hand, the global human body was modeled using lumped rigid bodies connected by proper joints. In addition, all the previous modeling studies considered mechanical impact loading rather than explosive loading. In this research, the pressure load is generated to the bottom of the vehicle by mine explosion. Pressure loading condition has rarely been conducted because of its unique military situation.

Table 4. The Classifications of Cervical Spine Injuries [Ref. 10]

Compression (vertical compression)
Jefferson fracure
Multipart atlas fracture
Vertebral body compression fracture
Burst fracture
Compression-flexion
Vertebral body wedge compression fracture
Hyperflexion sprain
Unilateral facet dislocation
Bilateral facet dislocation
Teardrop fracture
Compression-extension
Posterior element fractures
Tension
Occipitoatlantal dislocation
Tension-extension
Whiplash
Anterior longitudinal ligament tears
Disk rupture
Horizontal vertebral body fracture
Hangman's fracture
Teardrop fracture
Tension-flexion
Bilateral facet dislocation
Torsion
Rotary atlantoaxial dislocation
Horizontal shear
Anterior and posterior atlantoaxial subluxation
Odontoid fracture
Transverse ligament rupture
Lateral bending
Nerve root avulsion
Transverse process fracture
Other fractures
Clay shovelers' fracture

Oglesby [Ref. 12] investgated the effects of underwater explosion on ship's crew vulnerability. He used the articulate rigid body model to represent the human body. The technique applied for modeling the human body and its response is different, however his research is a good reference for this study considering as the model of indirect loading condition by external pressure.

Moisey and Dilip [Ref. 13] developed a finite element model for Side Impact Dummy (SID) in the test simulation for safety. Their research focused on the material selection in order to improve the predictable physical test results. They used the rubber or form-like materials. In their model, the number of elements of a SID was up to 16000, which requires great deal of computational time. Table 5 shows the detailed materials used for each part in SID.

Table 5. FEM Model of Side Impact Dummy [Ref. 13]

Body Part	FEM Model
Head	Skull- rigid shell Skin – viscoelastic solid elements
Neck	Solid elements made of hyperelastic rubber
Thorax	Ribs – several different materials depending on the locations ; solid steel ,solid urethane, damper, and solid foam
Lumber	Represented by rigid solid elements made of butyl rubber material
Pelvis	Pelvic bone- rigid butyl rubber shells Pelvic flesh – solid elements with foam material
Legs	Bones – rigid shell Flesh – solid

Belytschko, Schwer, and Privitzer [Ref. 14] modeled the human body as a collection of rigid bodies interconnected by deformable elements for the purpose of evaluating mechanical response in pilot ejection. The vertebral bones were represented by rigid body, while ligaments, muscles, and connective tissues were represented by deformable elements. The assumption for the treatment of bones as rigid bodies was that the stiffness of bones is normally greater than connective tissue. The followings are the models used in their human model: Rigid bodies for skeletal segments, spring element for ligaments, and beam elements for inter-vertebral discs.

III. FINITE ELEMENT MODEL

A. EXPLOSION PRESSURE

"The blast wave is generated when the atmosphere surrounding the explosion is forcibly pushed, as by the gases produced from a conventional chemical explosive, or as furnished by a volatilized container and components in a nuclear explosion" [Ref. 15]. The detonation of Anti-Personnel (AP) mine generates a hemispherical blast wave, and this blast wave can be considered as explosive shock. In order to model the explosive loads generated by an AP mine, two equations and one table (see Table XI) from Ref. [15] were used. The first equations is

$$Z = \frac{d * f_d^{\frac{1}{3}}}{W^{\frac{1}{3}}} \qquad (1)$$

where Z is the scaled distance from the detonation point, d is the actual distance, W is the TNT weight, and f_d is the distance factor. The weight of the explosive used in this research is 0.2kg which is equivalent to the main explosive charge of a PMN AP mine manufactured primarily by China. The distance factor f_d is found in Figure 10. If the explosion occurs within 500m altitude, the distance factor is close enough to one. [Ref. 15] The actual distance from the mine to the target was modeled as 20cm because of the buried depth of the PMN AP mine. When Z value is equivalent to 0.35m for the 0.2kg TNT, the pressure vs time curve used in this study was modeled from the table in [Ref. 15] and equation (2);

$$P = P_o(1 - t/t_d) \times e^{-\alpha t/t_d} \qquad (2)$$

where P is the ambient pressure, P_o is the peak explosion over-pressure, t_d is the duration time, and α is the wave form parameter. Figure 11 is the pressure load curve used in this research associated with a PMN AP mine. In the figure, Pa is the atmospheric pressure.

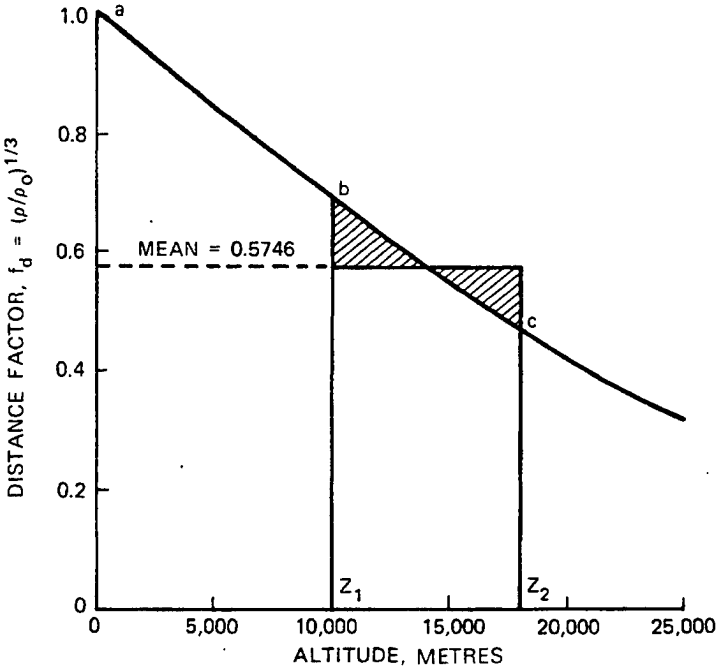

Figure 10. Mean Transmission Factor for Distance f_d [Ref. 15]

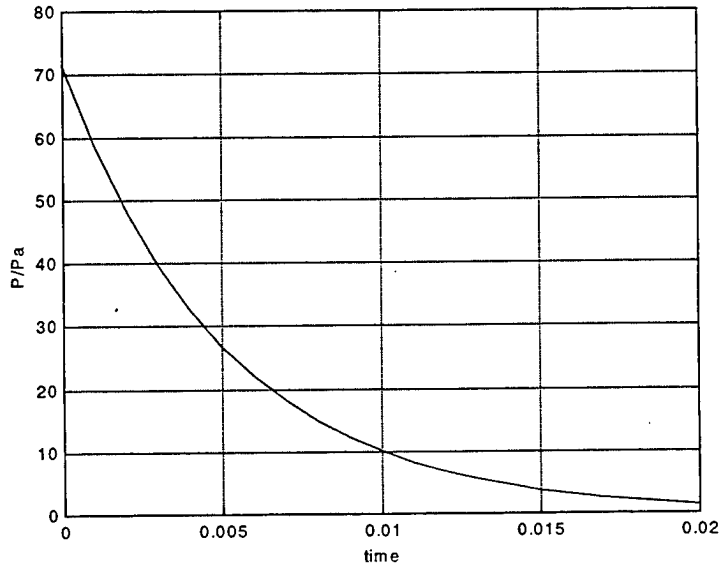

Figure 11. Load Curve Generated by the Explosion of a PMN Mine

B. HUMVEE

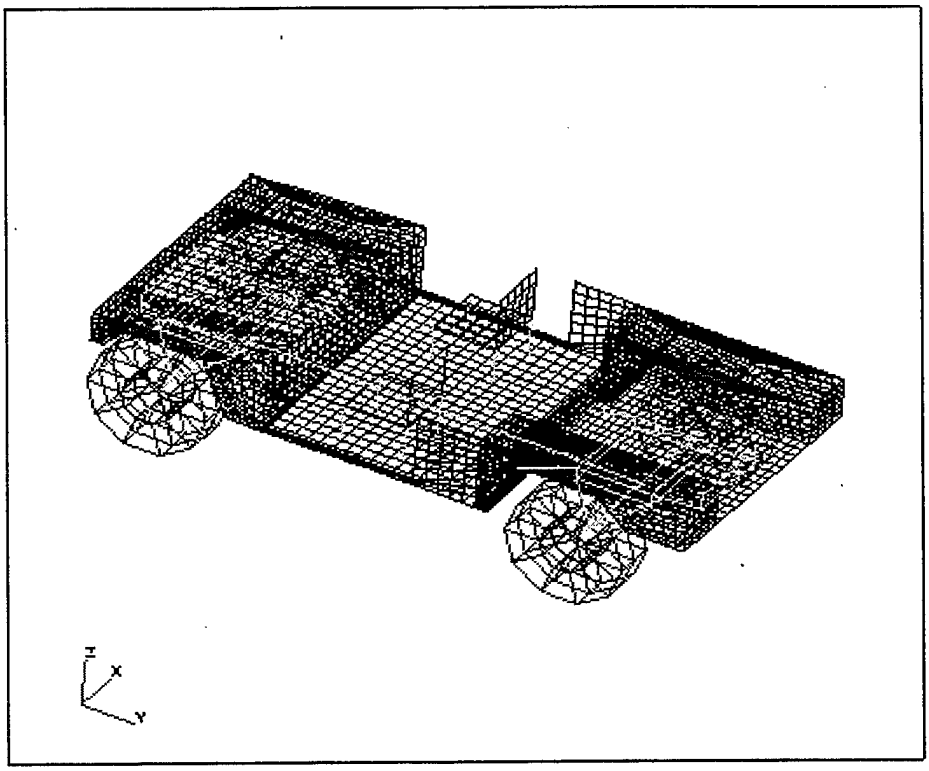

Figure 12. Finite Element Model of HUMVEE

The official name of the model used for this research is M1092A2 Base Platform. It is divided into 5 major parts, four identical wheels, two different beam sturctures, a body, two chairs, and one engine. The total number of elements and nodes are 4710 and 4670, respectively. The details of each material property and dimension will be mentioned in the following section. Overall specification of M109A2 Base Platform is in Table 5 given below.

Table 5. General Specification of M1092A2 Base Platform

Weight(kg)	Length(m)	Width(m)	Height(m)
2676	4.84	2.18	1.83

1. Wheel

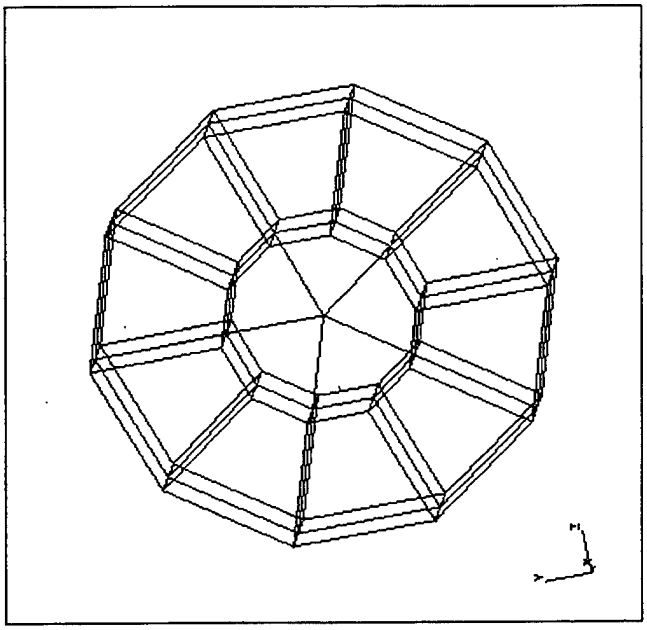

Figure 13. FEM Model of a Wheel

The vehicle consists of four identical wheels. Each wheel has 20 solid elements and 15 shell elements. The solid elements represent a tire, and the shell elements are used for the rim of the wheel. The material properties of the wheel model are given in Table 6.

Table 6. Material Properties of the FEM Model of the Wheels

Element	Material name	Elastic Modulus	Density	Poisson's Ratio
Solid	Polyethylene	4E+09 N/m	230 kg/cm^3	0.33
Shell	Steel	2E+11N/m	7800 kg/cm^3	0.3

2. Engine

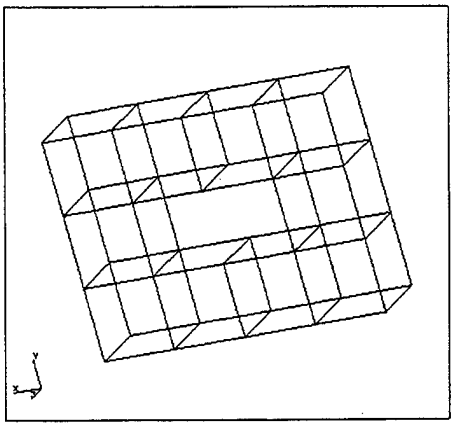

Figure 14. Simplified FEM Model of Engine

The engine block was simplified as 10 solid elements. Cast iron used for its material has an elastic modulus of 1.65E+11 Pa, density 6500 kg/cm^3, and Poisson's ratio 0.33. Outer dimension of the engine was $0.6\text{m} \times 0.8\text{m} \times 0.2\text{m}$.

3. Vehicle Body

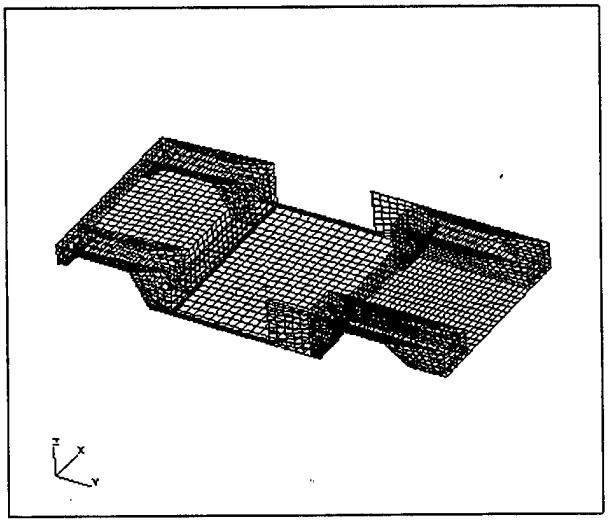

Figure 15. FEM Model of the Vehicle Body

The vehicle body was made of thick steel (0.35 cm), which has 2700 kg/m^3 density, 69 GPa elastic modulus, and 0.29 Poisson's ratio. This FEM model for the vehicle body consisted of 4062 nodes, 4120 aluminum shell elements, and 8 spring beam elements. Those beam elements were used to connect the vehicle body to the frame structure.

4. Frame

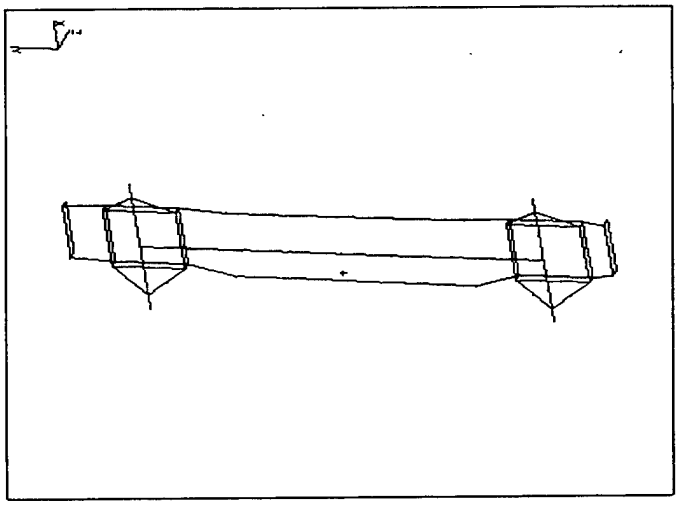

Figure 16. FEM Model of Vehicle Frame

In addition to the frame itself, the frame structure also includes a transmission, axle shafts, and a drive shaft. Beam elements were used to represent those subparts. Eight spring elements and 8 damper elements were also used simultaneously to represent actual springs and shock absorbers. The frame consisted of a rectangular hallow beam and shafts and the transmission were modeled using cylindrical beams. The cylindrical elements had a 0.2m diameter for the transmission and the housing. The total number of nodes and elements in the entire frame structure were each 57 and 86. Steel was used for the material. The cross sectional shapes and dimensions of beam elements for the frame and the axles are shown in Figure 17.

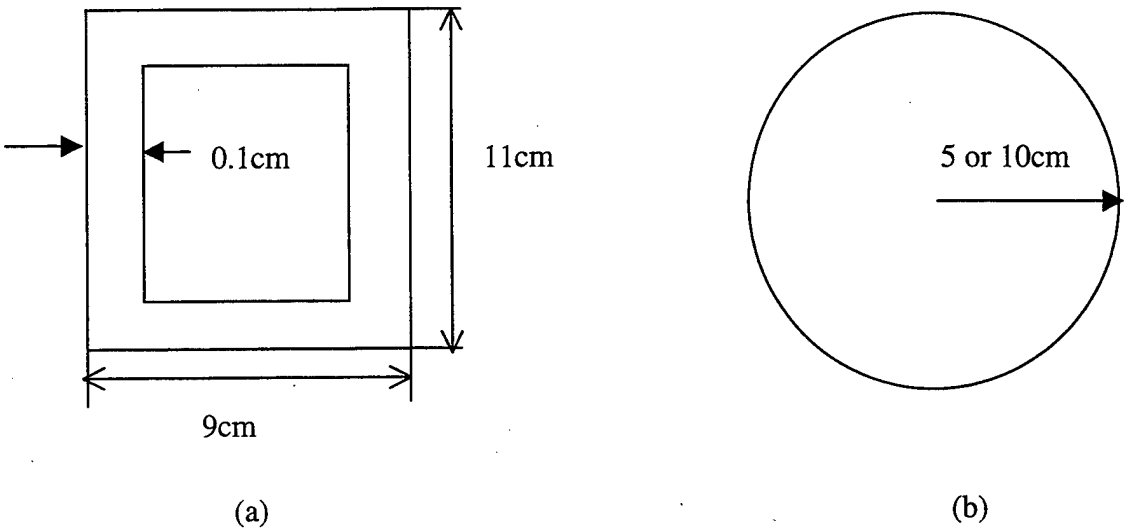

Figure 17. The Cross Sectional Dimensions of Beam Elements for (a) Frame (b) Transmission (10cm) and Axle (5cm)

5. Chair

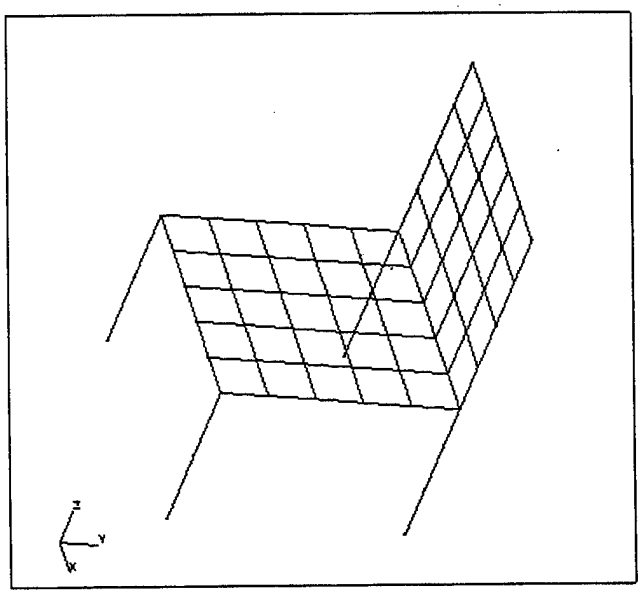

Figure 18. FEM Model of a Chair

There were two chairs in the model consisting of four legs with two beam elements and two plates consisting of shell elements. A thick aluminum, 0.5cm thick, was used for chair plates and cylindrical aluminum beams were used for chair legs. The chair had 46 shells and eight beam elements.

C. HUMAN BODY

The objective of this research was to evaluate the biomechanical response of the human body inside a military vehicle exposed to mine explosion. Therefore, the FEM modeling of the human body was critical for this in this research. However, it was very difficult to model the details of the human body because of its complex geometry, material property, and wide variation from person to person.

King [Ref. 16] investigated the biomechanical response of the human head and cervical spine due to impact on a ballistic protective helmet. He developed a model for the cervical spine and head. The human body model used in this research was based on King's model and extended for the entire body, as shown in Fig. 19.

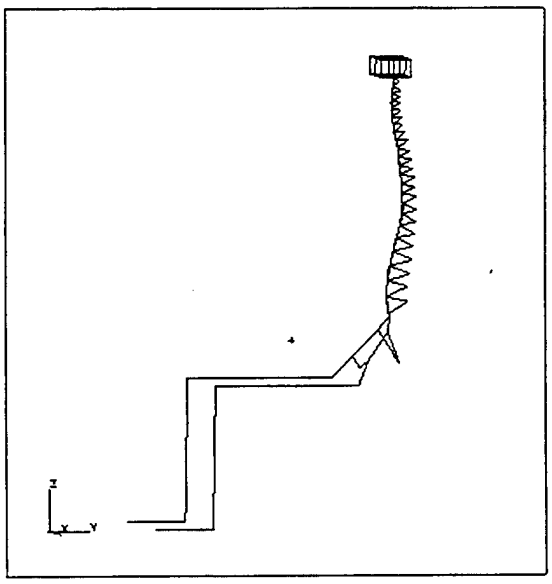

Figure 19. FEM Model of a Human Skeleton Body Seated on a Chair

1. Head

The focus of the head model is given to provide proper mass and center of gravity of the head, since we are interested in brain injuries caused by head acceleration. The head consisted of six solid elements with 24 nodes.

2. Spine

King [Ref. 16] modeled spines as follows; each cervical vertebra by two beams, a vertebral disk between each vertebra by a single beam, the facet joints by two beams extending from the midpoints of adjoining vertebra, and the connection between them by a discrete beam. LS-DYNA [Ref. 15] defines the discrete beam element for simulating the effects of a linear elastic zero length beam by using six springs each acting about one of the six local degrees of freedom. Each spring constant was adjusted depending on its allowable movement. Another important point of this model was to model the numerous ligaments around the spine. They were reduced to a single ligament running from C1 to L5. The ligament was modeled using a cable element, since it can only resist to a tensile force. The above modeling concept was extended to the entire spine model including cervical, thoracic, and lumbar.

3. Other

The human body in this model was posed as seated on a chair of a vehicle. Legs (tibias and femurs), sacrum and tarsus were modeled using beam elements. For the body joints among them, discrete elements were used with proper constraints in their motions, respectively. Hence, care was given to each directional stiffness value. That is, a high stiffness value restricts the translational or rotational motion of a respective joint to the given direction. Ribs, clavicle, scapula, and arms were not included in this model.

IV. INJURY CRITERIA

There are no universal standard to evaluate injury potential of the human body caused by external loading, since everyone is different in size, strength, and even response to the same loading conditions. Differences also arise from sex, age, and body posture. However, consistent demands for evaluating injuries and protecting the human being from injuries were motivated and resulted in some injury criteria and reference values, which have been commonly used in the aerospace and automobile industry for safety. Injury Assessment Reference Values (IARV's) developed by General Motors in the early 1980's and the Head Injury Criteria (HIC) based on an average value of the resultant acceleration of the head have been widely accepted. Furthermore, there are several other published critical injury values for various injury modes of the human being.

A. BRAIN INJURY

The Head Injury Criterion is defined as:

$$HIC = \left[\left(\frac{1}{t_2 - t_1} \right) \int_{t_1}^{t_2} a(t)dt \right]^{2.5} (t_2 - t_1) \qquad (3)$$

where a is the resultant acceleration of the center of mass of the head in gravity G's and (t_2-t_1) is the time interval in seconds between any two points in the time history of a node. To apply this equation, care should be given to the time interval, since a large time interval results in an unrealistic high HIC value. There are two guidelines for the time interval; the Federal Motor Vehicle Safety Standard (FMVSS) 208 of United States limits the maximal time interval to 36 msec. while the International Organization for Standardization (ISO) has chosen 15 msec. as the limit [Ref. 14]. These values were used with the HybridIII male dummy. The ISO guideline was adopted in this study

Another important factor associated with the HIC value is the Abbreviated Injury Scale (AIS). HIC has several injury scales to predict the injury. AIS is used to classify the

level (severity) and potential of injuries. AIS was developed by the Association for Advances of Automobile Medicine in early 1970's. Table 5 shows the AIS levels.

Table 7. Abbreviated Injury Scale Severity Codes [Ref. 18]

AIS	Severity Code
1	Minor
2	Moderate
3	Serious
4	Severe
5	Critical
6	Virtually unsurvivable

That is, the HIC value computed using Eq. (3) indicates the injury risk associated with AIS for the brain injury. Figure 10 shows the possibility of risk of the head injury at least AIS level 4 based on the ISO guideline.

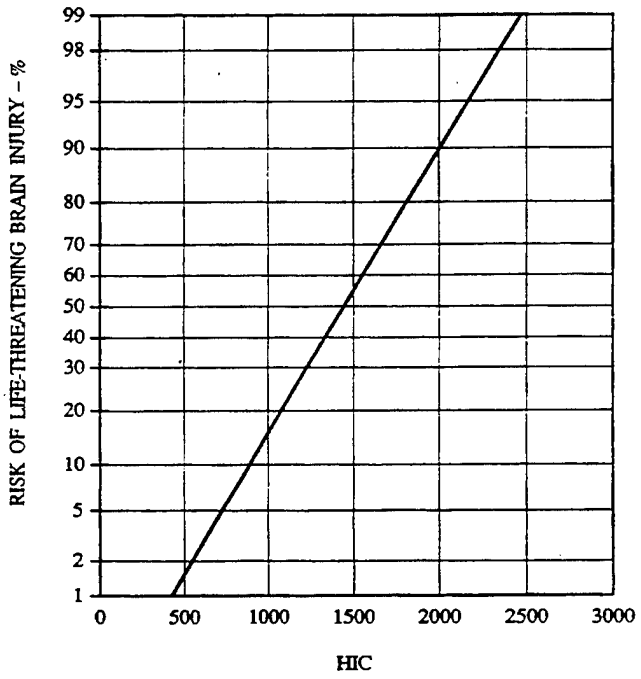

Figure 20. Injury Risk Curve for HIC [Ref. 19]

B. INJURY TO THE CERVICAL SPINE AND OTHERS

Before dealing with the spinal injury assessment, an additional description should be provided. For example, the description of extension and flexion depends on the initial position of the head and neck at the moment of loading, since extension and flexion are relative motions among head, neck, and torso. Figure 21 describes the nomenclature of the motions between head and neck, and the engineering description of spine loading.

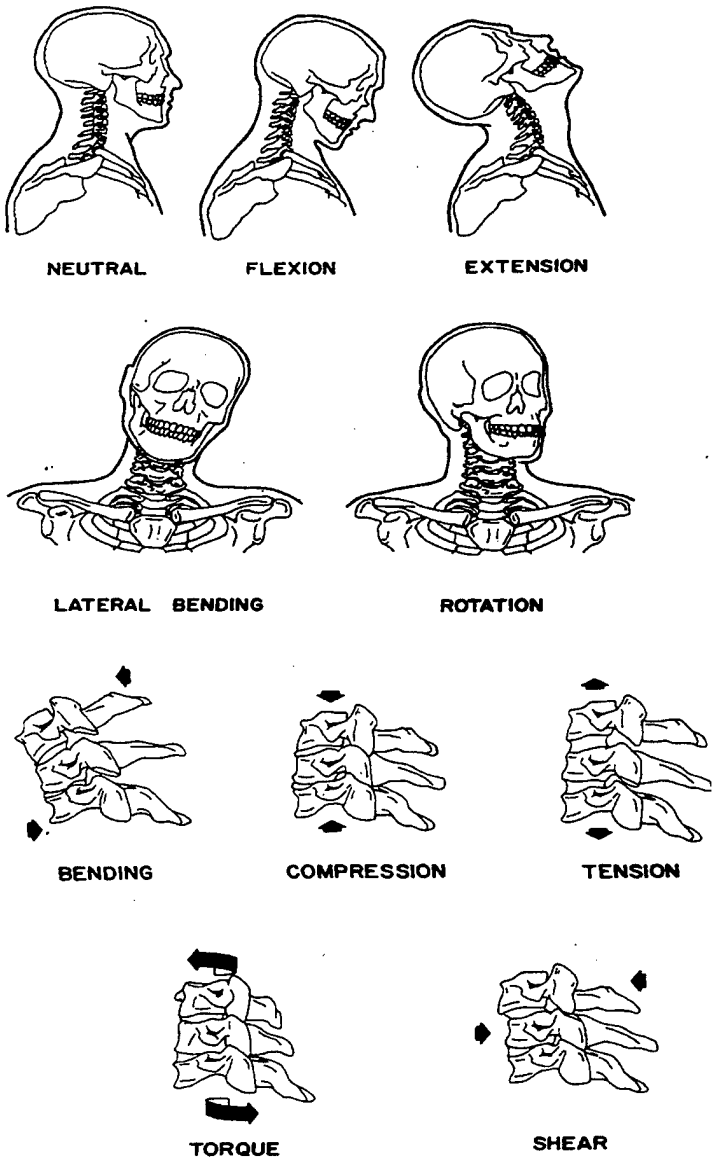

Figure 21. Description of Head Motion and Description of Neck Loading [Ref. 10]

In addition to the classified description of spinal injury, configuring the injury mechanism will be another important challenge in its evaluation. "Purely compressive loading of the cervical spine occurs infrequently due to the complexity of the structure."[Ref 10] Even if the applied loading condition is axial compression, the resultant loading will be different for each ligament, vertebra, or disc. The types of loading for injuries to the cervical spine are divided into compression, compression-flexion, compression-extension, tension, tension-flexion, tension-extension, torsion, horizontal shear, and lateral bending [Ref. 10]. Figure 22 and 23 show an example of neck injury mechanism under different loading conditions.

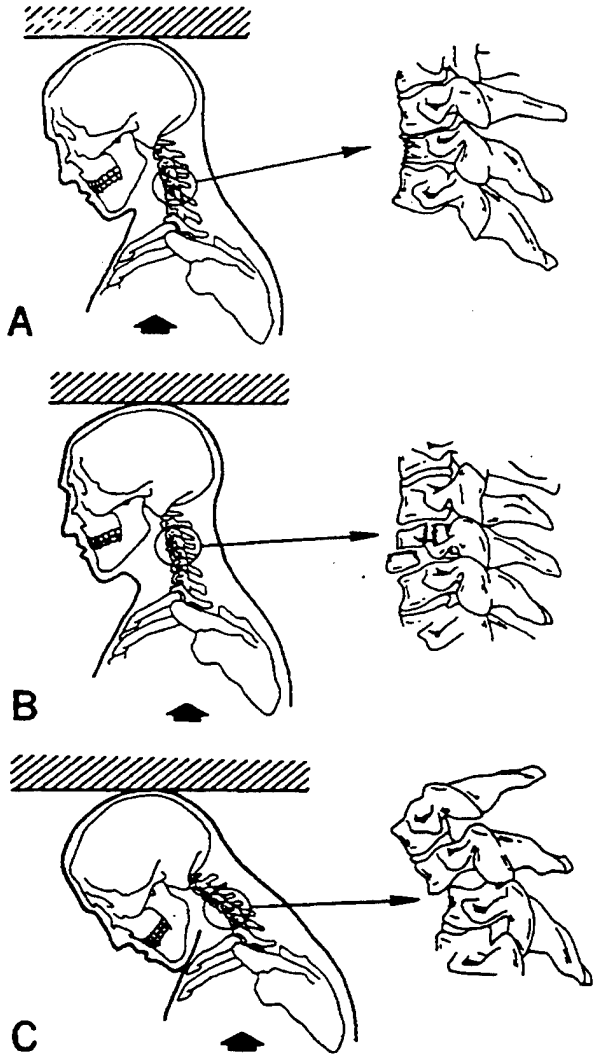

Figure 22. Flexion-Compression Injury Mechanisms [Ref. 10]

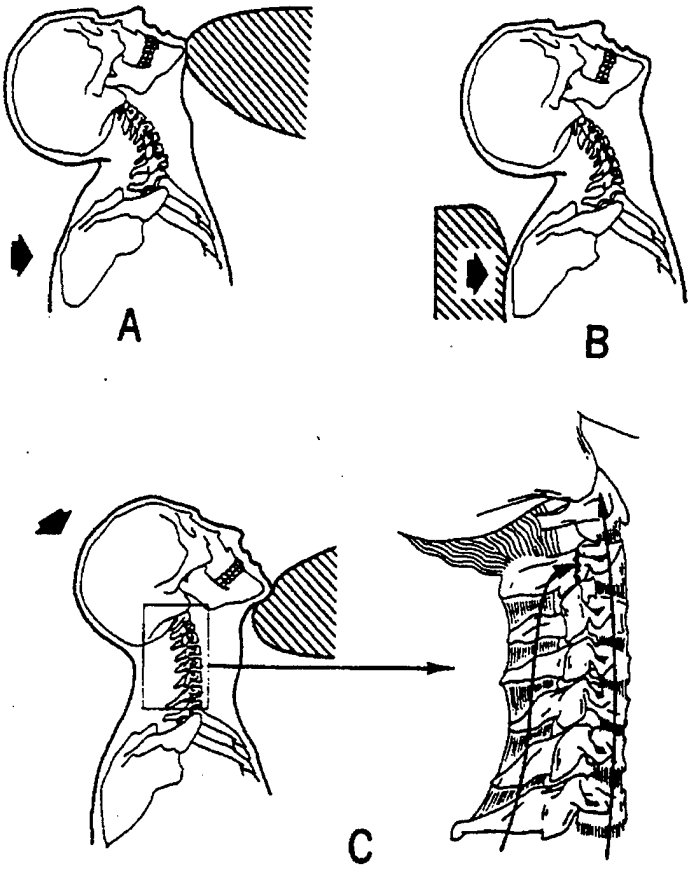

Figure 23. Tension-Extension Injury Mechanisms [Ref. 10]

Evaluating injuries to the cervical spine was undertaken by comparing the critical tolerance values under various loading conditions with the calculated values. However, the tolerance value associated with each loading condition also varies because of the variation of the spinal properties, the posture upon loading, etc. Following IARV's, Table 8 and Figures 24-26 provide guidelines for assessing injury potentials for each body section measured from Hybrid III type adult dummies [Ref. 10]. Table 9 summarizes the tolerance levels of the cervical spine in order to evaluate injury potential under the specific loading conditions of this study. IARV's for the femur, tibia, and foot are provided in Table 8.

Table 8. Injury Assessment Reference Values for Hybrid III-Type Adult Dummies [Ref. 10]

Body region Injury-assessment criteria[a]	Small female	Midsize male	Large male
Head			
HIC; $(t_2 - t_1) \leq 15$ ms	1,113	1,000[b]	957
Head/neck interface			
Flexion bending moment (Nm)	104	190	258
Extension bending moment (Nm)	31	57	78
Axial tension (N)		Fig.24	
Axial compression (N)		Fig.25	
Fore/aft shear (N)		Fig.26	
Chest			
Spine box acc.; (3 ms, G)	73	60	54
Sternal deflection due to:			
— Shoulder belt (mm)	41	50	55
— Air-bag & steering-wheel hub (mm)	53	65	72
Viscous criterion (m/s)	1	1	1
Femur		Fig.27	
Axial compression (N)			
Knee			
Tibia-to-femur translation (mm)	12	15	17
Med./lat. clevis compression (N)	2,552	4,000	4,920
Tibia			
Axial compression (N)	5,104	8,000	9,840
Tibia index, $TI = M/M_c + F/F_c$	1	1	1
Where,			
M_c—critical bending moment (Nm)	115	225	307
F_c—critical comp. force (kN)	22.9	35.9	44.2

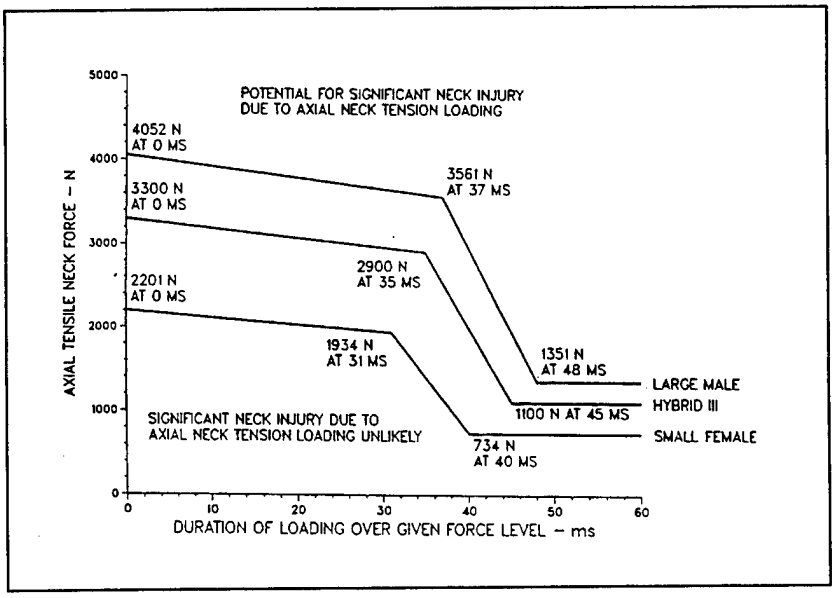

Figure 24. Injury Assessment Curves for Axial Neck Tension [Ref. 10]

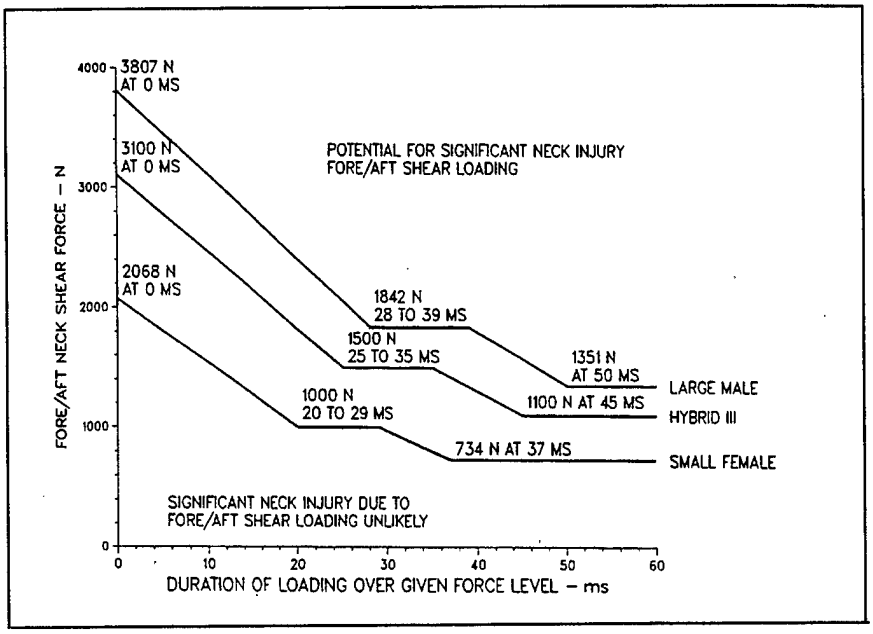

Figure 25. Injury Assessment Curves for Axial Neck Compression [Ref. 10]

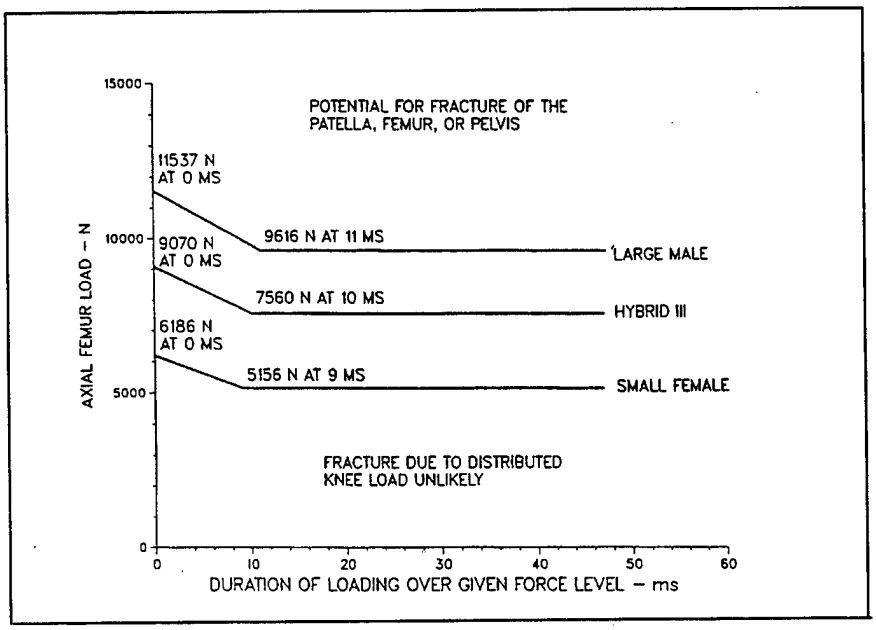

Figure 26. Injury Assessment Curves for Axial Compressive Femur Force [Ref. 10]

Table 9. Summary of Injury Tolerance Levels to the Cervical Spine

Injury Type	Loading condition	Value	Source
Ligamentous Injury	Tension	76 N	Ref. 4
Facet Dislocation	Compression	1720 N	Ref. 10
Disc injury	Compression	74 N	Ref. 4
	Torsion	1.8 N-m	
	Bending	11 N-m	Ref. 21
Vertebra injury	Compression	3620 N	Ref. 21
	Bending	19.6 N-m	

V. RESULTS AND DISCUSSION

Varying conditions were used to compare results from two simulations. The first simulation was performed for the original model of the vehicle. Potential injury of the human body was investigated with different perspectives associated with various injury criteria. Head injuries were examined based on the nodal acceleration of the head. For neck injury evaluation, it was important to examine critical information, such as the type of loading (axial, shear, bending or torsional loads), their peak values and corresponding locations. In particular, separate injury criteria was applied to the vertebra, disk, ligament, and facet joint. Even if every component of the cervical spine from C1 to C7 was investigated, this study showed that the discs, vertebrae, facet joints, and the ligaments between C4 and C5 inclusive were most critical in terms of injury potential. For the femur, the axial load was considered. The computer simulation continued up to 1.2 sec. since most peak values occurred just after 1 sec.

The second test was conducted with a modified vehicle. The modified model had dampers at the legs of the chair inside the vehicle in order to reduce the injury potential. It was also analyzed using the same criteria as used for the first model. The following sections describe the detailed results of simulation and give the comparison between the two models.

A. INITIAL MODEL

1. Response to HUMVEE

Figures 27-32 show the displacement and deformation of the vehicle body in chronological order from 0 second to 0.8 second. The mine explosion was just below the right front tire. The red color fringe represents a larger deformation. As expected, the shock wave propagated from the right front of the vehicle where the explosion occurred. The overall deformation was not significant over the entire vehicle because there was rigid body rotation of the vehicle. However, the front half of the vehicle was twisted relative to the other half caused by the shock wave. Figure 32 shows that the vehicle eventually capsized by the explosion.

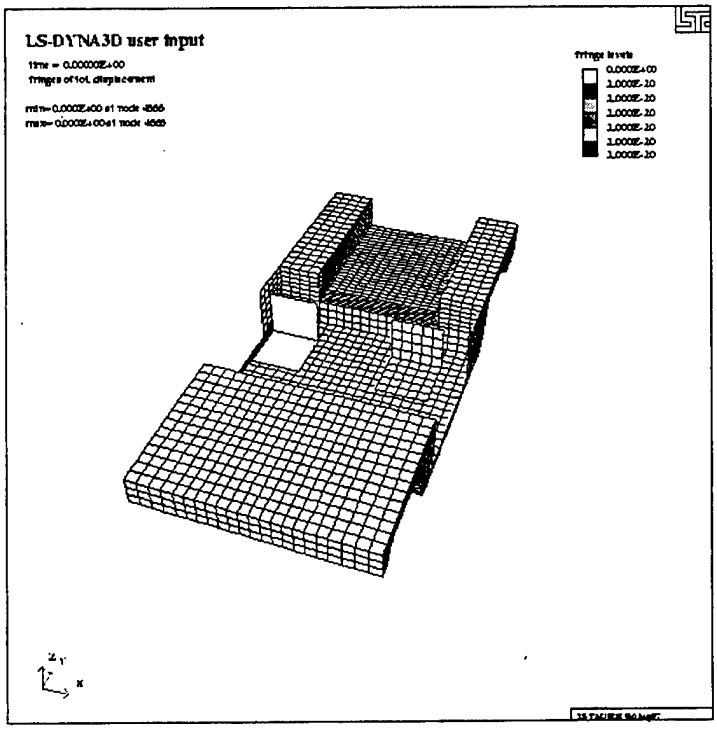

Figure 27. Initial State of the Vehicle

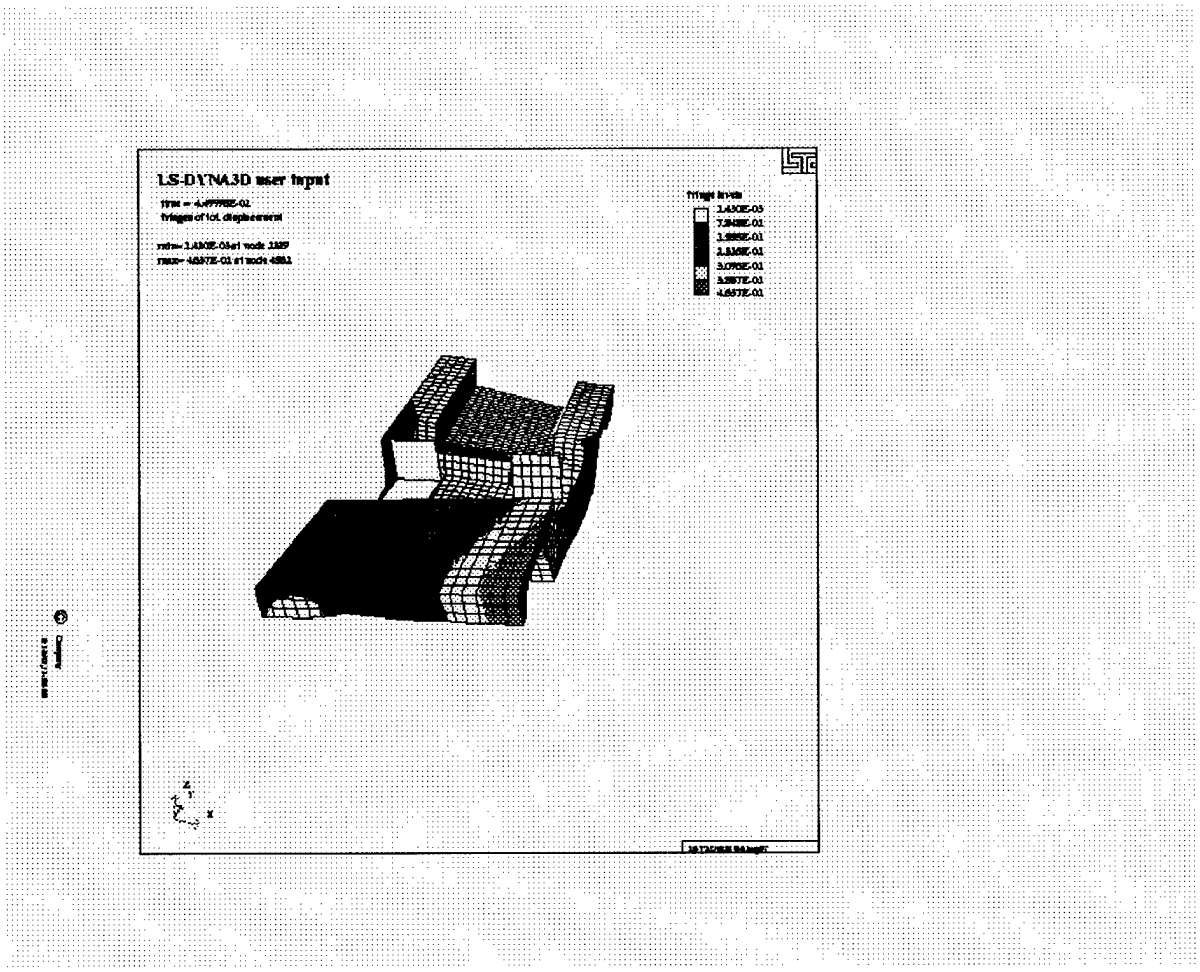

Figure 28. Displacement of the Vehicle 0.05 Second after Explosion

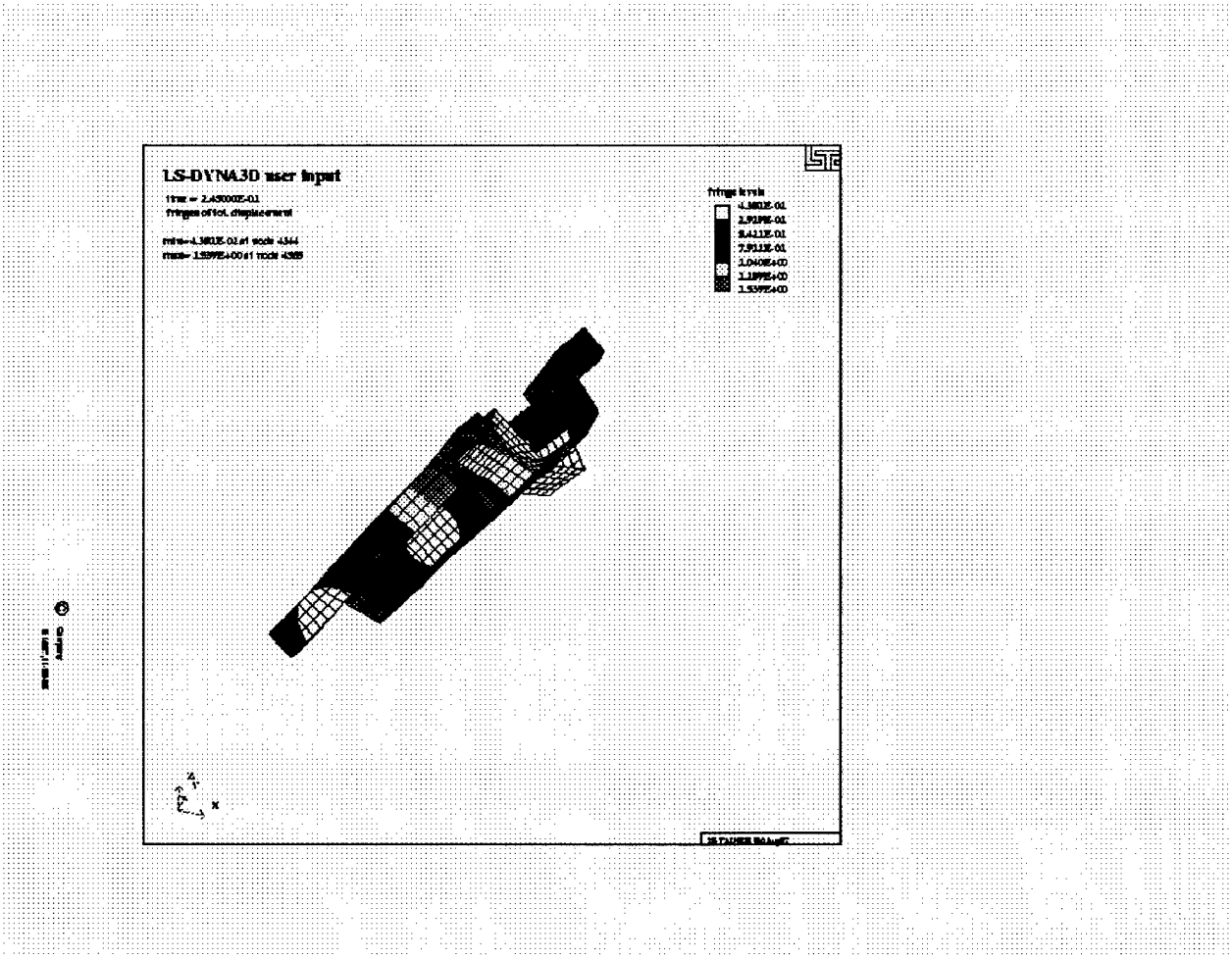

Figure 29. Displacement of the Vehicle 0.24 Second after Explosion

Figure 30. Displacement of the Vehicle 0.5 Second after Explosion

2. Human Body Response

a. Brain Response

The maximum acceleration of the head center was 699G at 1.153 sec after the explosion, as shown in Fig 31. The calculated maximum HIC value using Eq. (3) for the period of 15 msec was 9108. This value, when compared to the head injury curve shown in Fig. 20, suggests that there is an extremely high probability of life-threatening brain injury, including death of the onboard crew. The calculated HIC value was nine times higher than the commonly selected tolerance value of 1000. The HIC value 1000 means that approximately 16% of human beings exposed to the acceleration are injured over an AIS level 4 [Table 7].

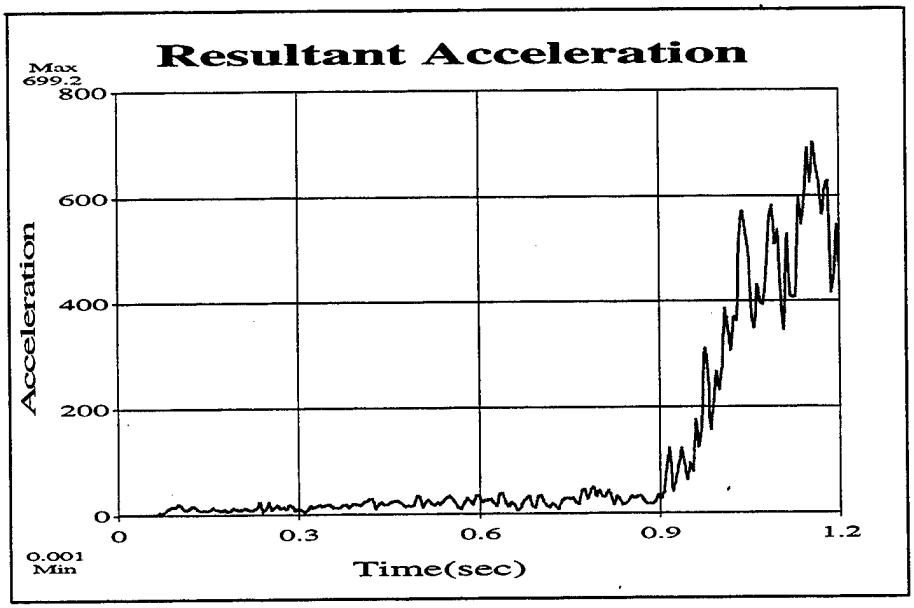

Figure 31. Resultant Acceleration at the Center of Head

b. Responses at the neck and the femur

Figures 32-34 show the resultant bending moment, compression force, and torsional moment at the disc between C4 and C5. The maximum value of all three loads from the plots exceeded their corresponding injury tolerance level. The calculated bending moment was 26.3 N-m, which was approximately two times greater than the

tolerance value of 11 N-m. The compressive force on the disk far exceeds the tolerance value implying disk fracture. As shown in Fig. 34, the computed maximum torsional moment was 9.5 N-m which also exceeds the tolerance value of 1.8 N-m. In summary, the analysis indicated disk rupture under the given mine explosion.

For the ligament, the response to the tensile force was considered because of the cable-like behavior of the component. The resultant tensile force at the ligament between C4 and C5 was almost negligible for this case (see Fig.35). The vertebra was strong enough to withstand the compressive force, however, the maximum resultant bending moment at the vertebra of C4 was 65.32 N-m. This value is 3.5 times higher than the tolerance level of the vertebra (see Fig. 36-37).

In this study, the failure at the facet joint caused by the shear force or lateral bending was unlikely because the loads were negligible compared with others. Figure 38 shows the resultant compressive forces at the facet joint between C4 and C5. The injury criteria expects that the facet dislocation occurs at 1720 N. The maximum resultant compressive force, 1479 N from Figure 38, was lower than the injury criteria.

Figure 39 indicates that the possibility of femur fracture is very low. The maximum force on the femur was 1740 N, while the fracture strength was 5160 N, even for an average small female.

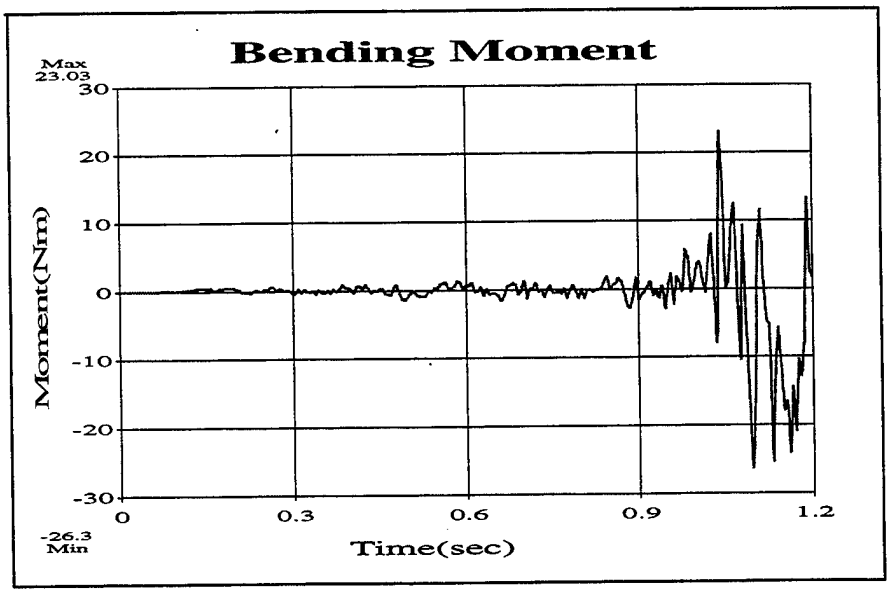

Figure 32. Bending Moment at the Disc between C4 and C5

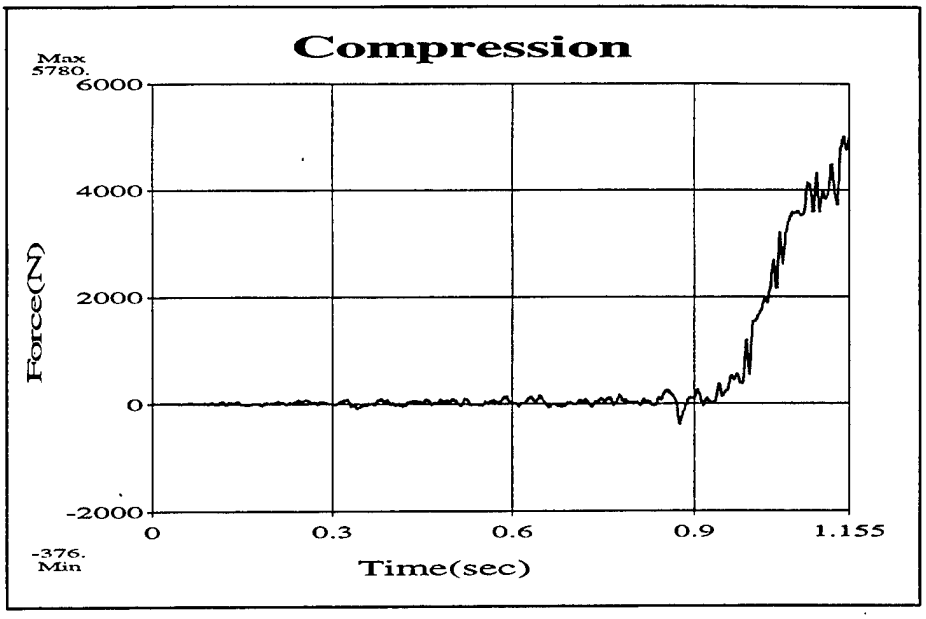

Figure 33. Compression Force at the Disc between C4 and C5

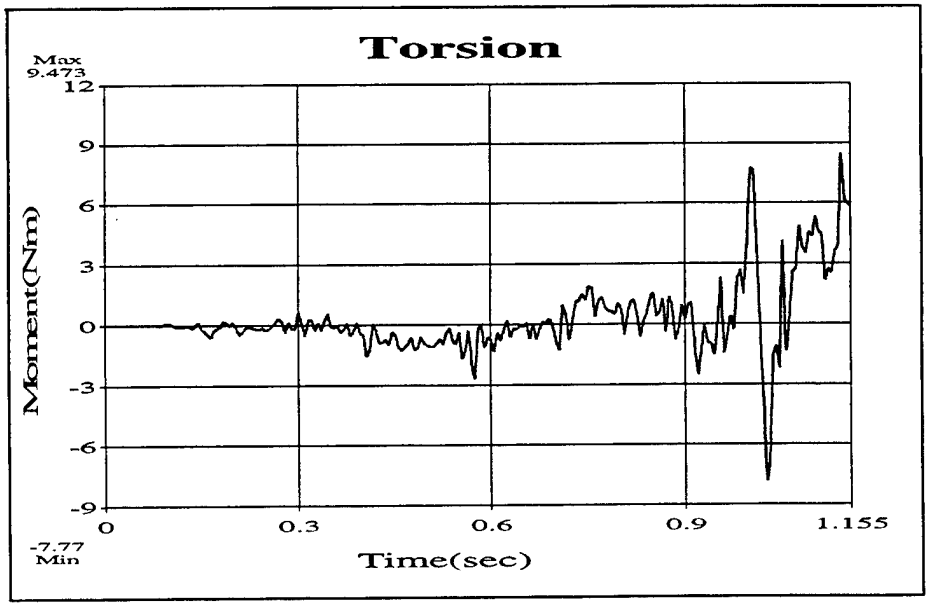

Figure 34. Torsional Moment at the Disc between C4 and C5

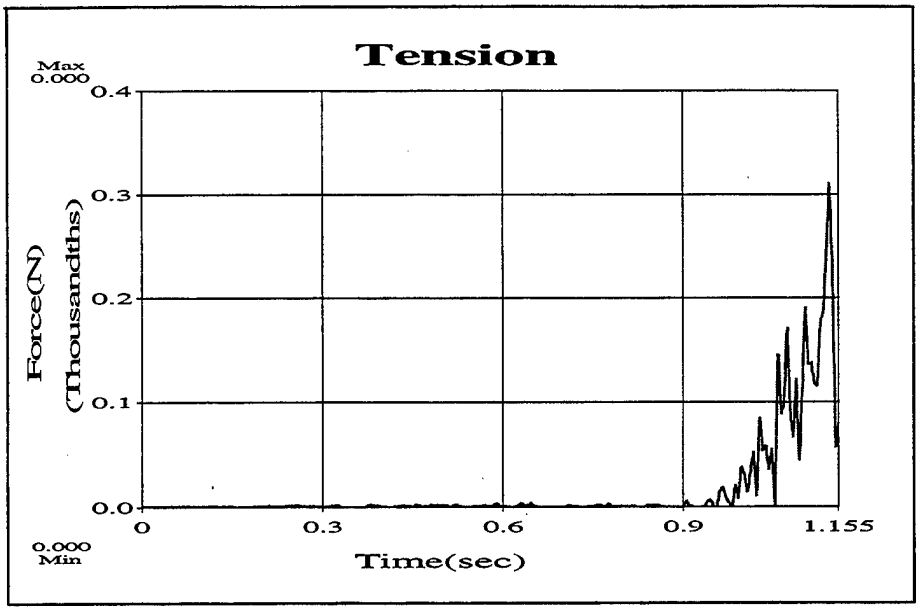

Figure 35. Tension at the Ligament between C4 and C5

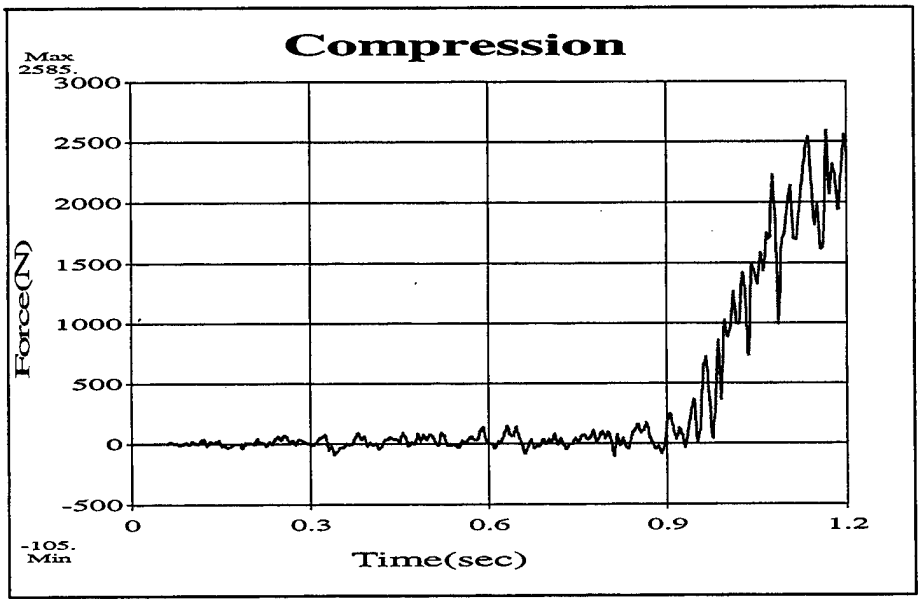

Figure 36. Compression at the Vertebra C4

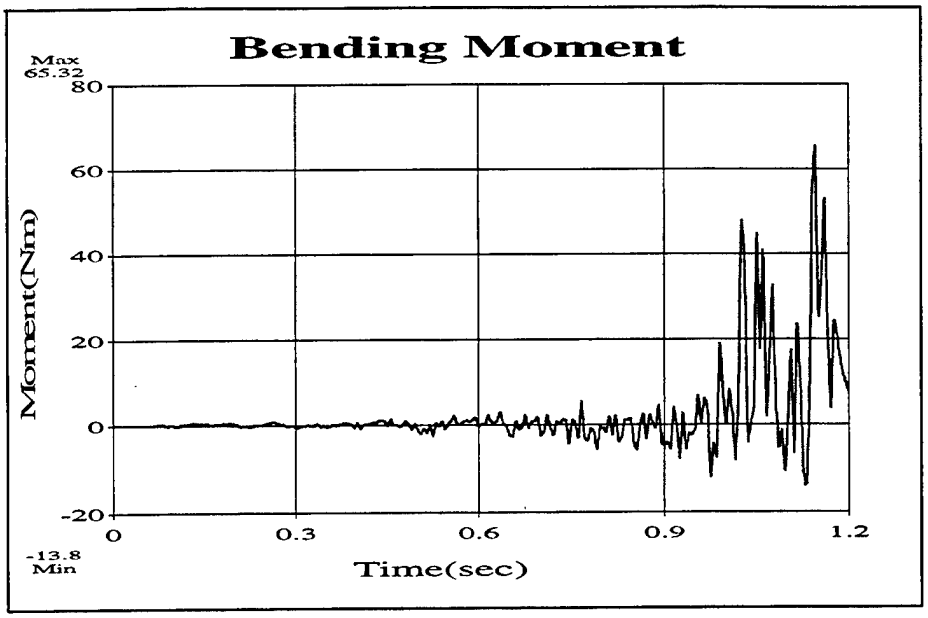

Figure 37. Bending Moment at the Vertebra C4

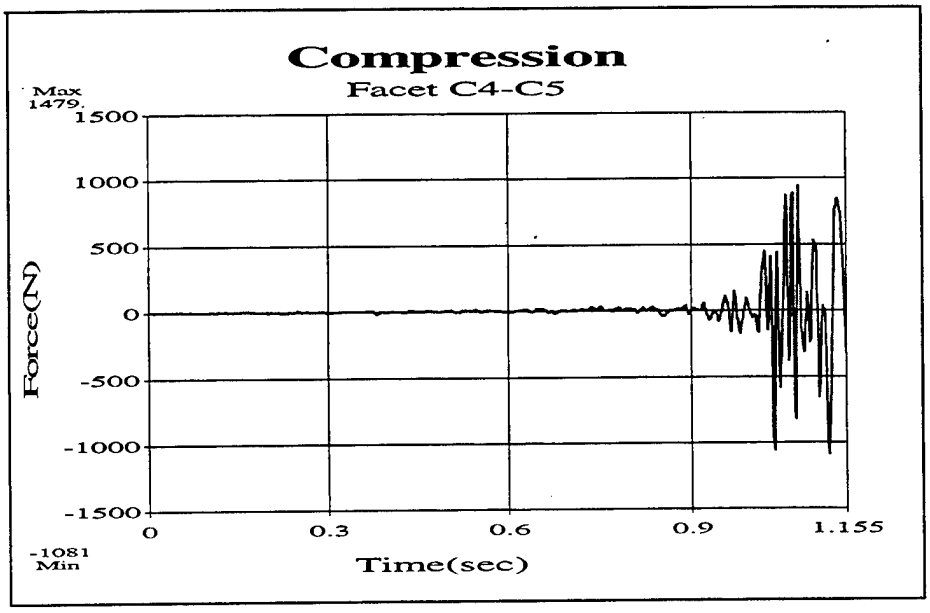

Figure 38. Compression at the Facet Joint between C4-C5

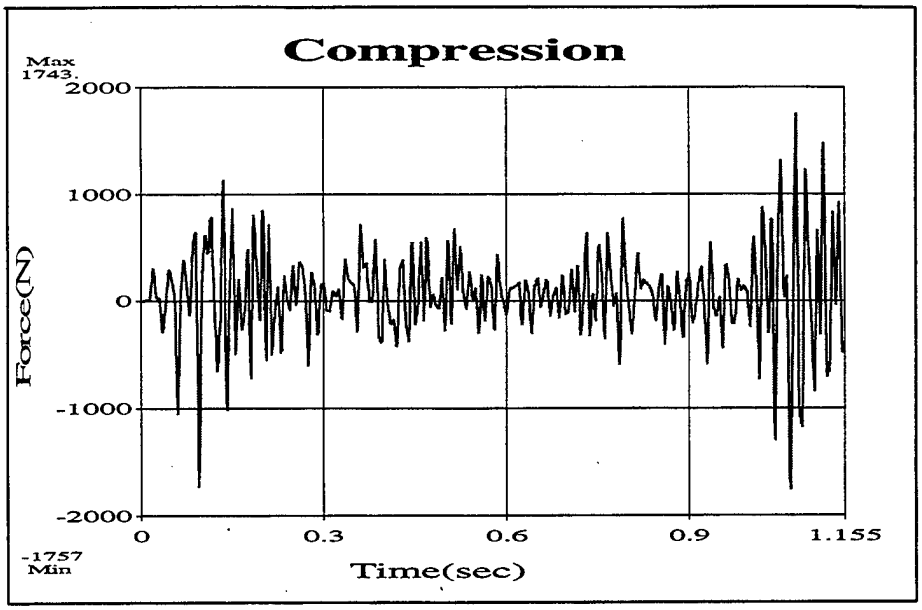

Figure 39. Compression at the Femur

B. MODIFIED MODEL

The modification of the original model reduced the overall resultant acceleration at the head and transferred loads to the neck. Adding dampers particularly decreased the axial compression of the spinal components. There was little difference between the maximum peak values of acceleration of both models at the head center. However, the duration of the peak acceleration was greatly reduced for the modified model (see Fig.40). As a result, the HIC value of the modified model was about 25% less than the original model. The HIC value of the modified model was 7043 and was still too high for safety.

Figures 41-43 show that the modified model reduced resultant loads transferred to the vertebral discs significantly. In particular, the axial compressive force on the disc between C4 and C5 was dramatically reduced. However, the calculated values of the modified model were still much greater than the tolerance values for the compressive load as well as the torsional moment. On the other hand, the maximum bending moment from Figure 41 became comparable to the tolerance level of the disc.

As far as vertebra injury was concerned, the bending moment was reduced by a factor of 3 when compared to that of the original model (see Fig. 44). The reduced bending moment became slightly greater than the injury tolerance value. Figure 45 shows the compressive force at the vertebra.

For the facet joint, the compressive force was also decreased more than half and the force was much lower than the tolerance value (see Fig. 46). The load transferred to the femur barely changed between the two models (see Fig. 47).

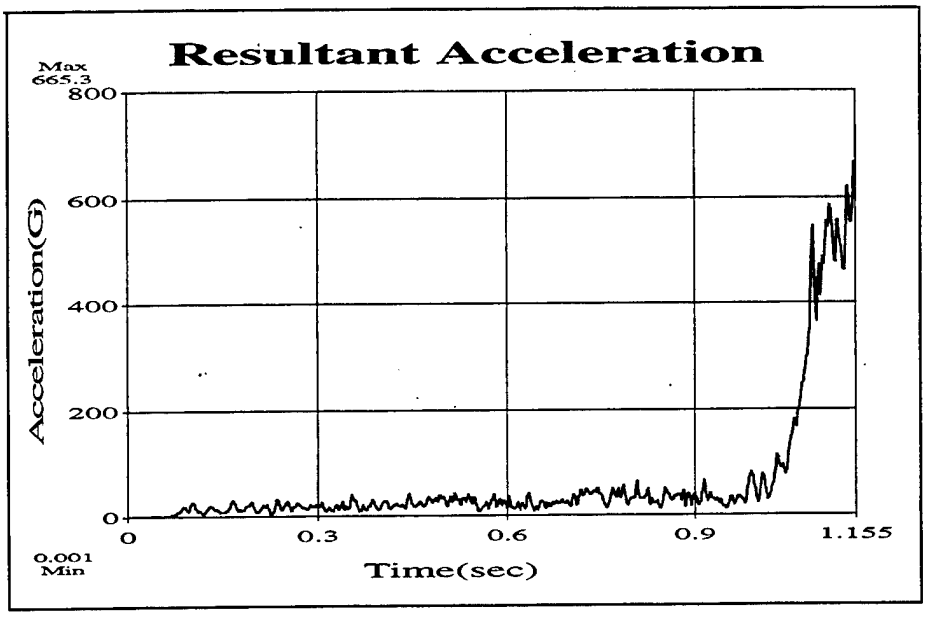

Figure 40. Resultant Acceleration at the Center of Head for the Modified Vehicle

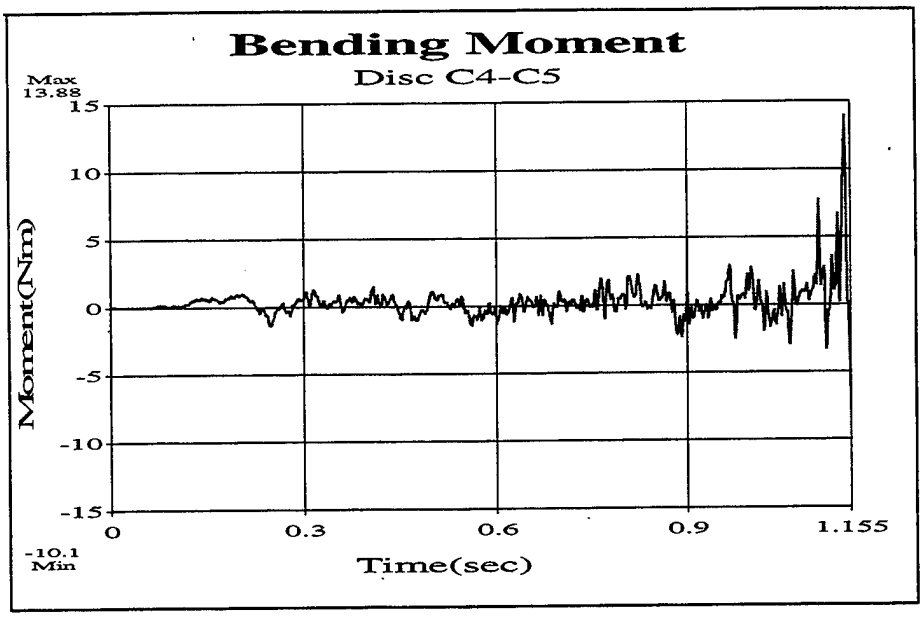

Figure 41. Bending Moment at the Disc between C4 and C5 for the Modified Vehicle

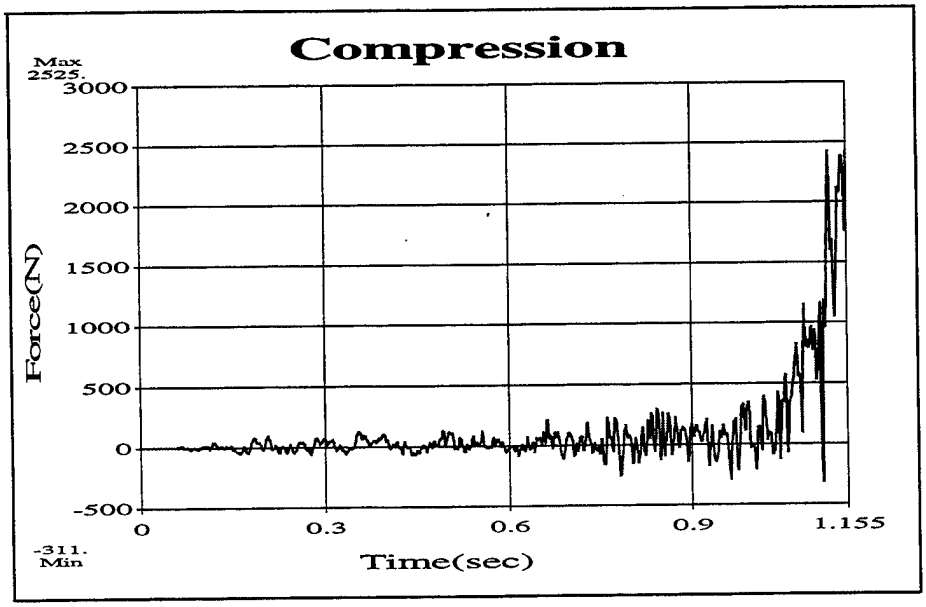

Figure 42. Compression at the Disc between C4 and C5 for the Modified Vehicle

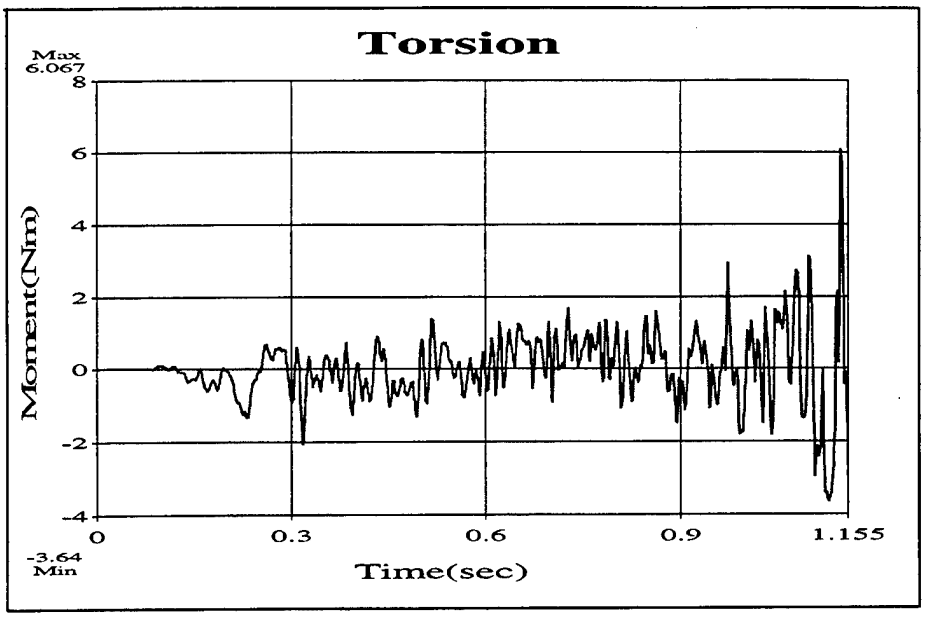

Figure 43. Torsional Moment at the Disc between C4 and C5 for the Modified Vehicle

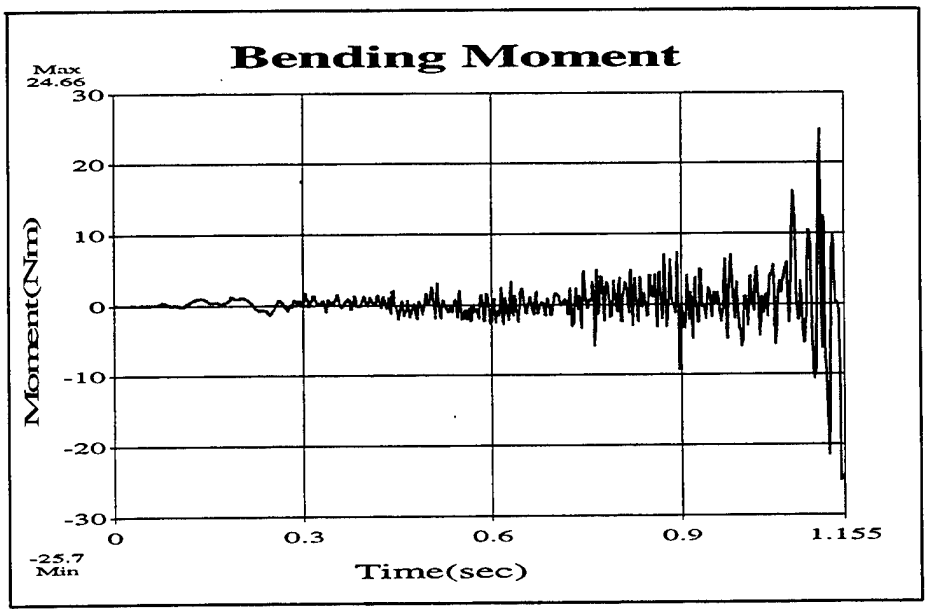

Figure 44. Bending Moment at the Vertebra C4 for the Modified Vehicle

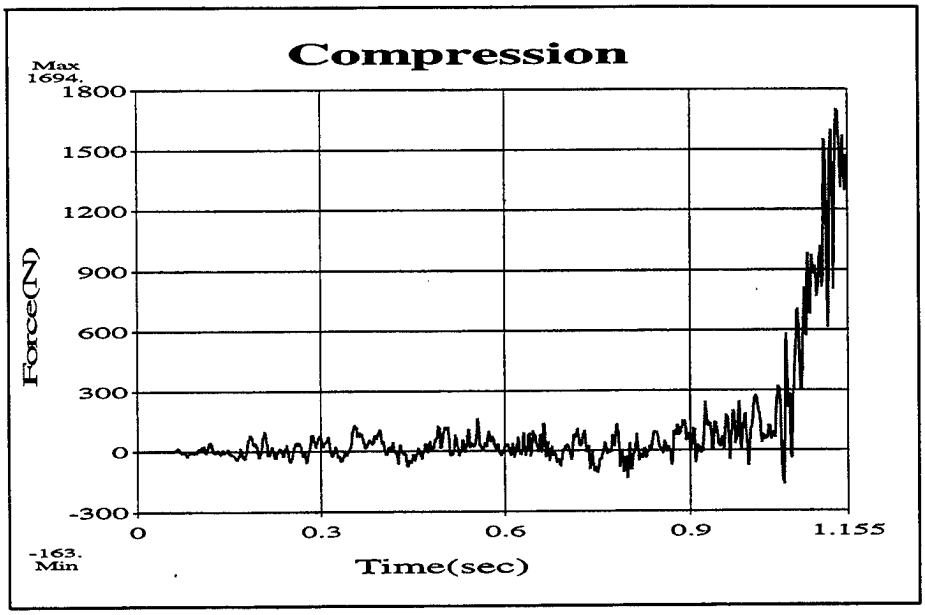

Figure 45. Compression at the Vertebra C4 for the Modified Vehicle

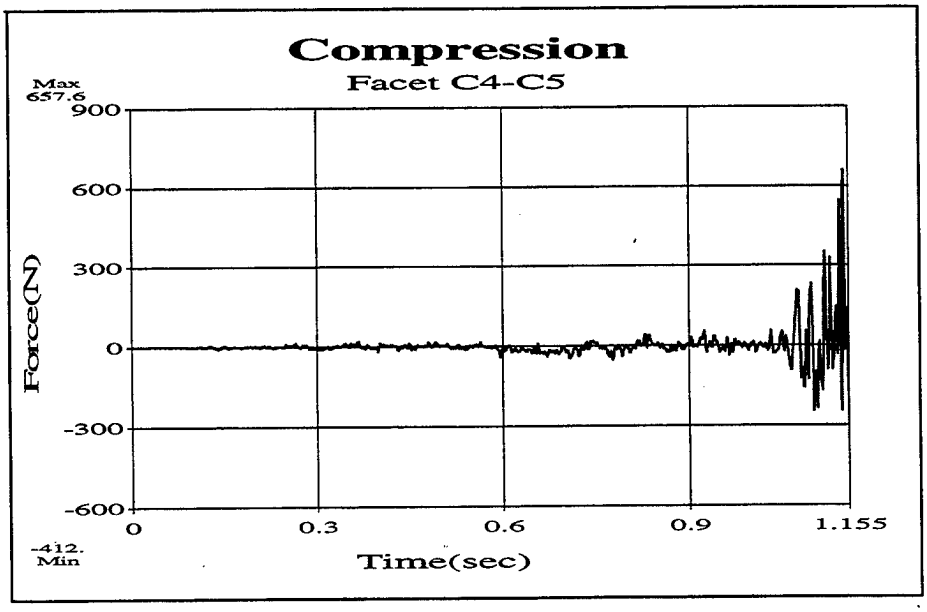

Figure 46. Compression at the Facet joint between C4 and C5 for the Modified Vehicle

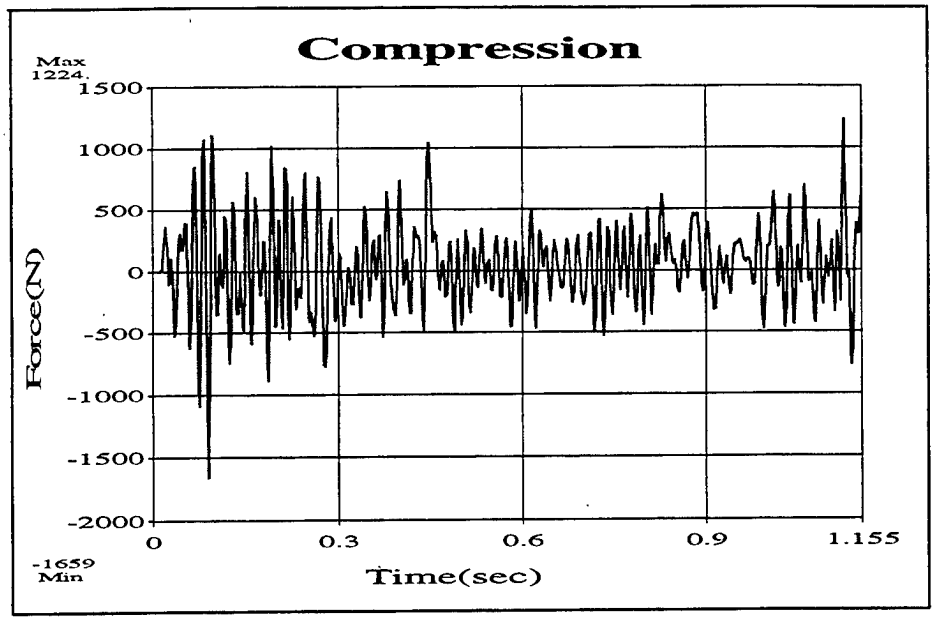

Figure 47. Compression at the Femur for the Modified Vehicle

C. SUMMARY

Comparison of the results from the two models was made and summarized in Table 10. The commonly used tolerance value for respective injury mode was also tabulated. In Figures 48-51, time-history plots of different loads and the head acceleration were also compared between the original and modified model.

In general, the modification significantly reduced the loads and the duration of peak acceleration.

One thing to be noted is that when the calculated values are greater than the tolerance values, injury is not definite. The tolerance values should be interpreted as more or less a guideline, since the values can vary significantly from person to person depending on many varying factors. However, one can say that the injury potential is definitely reduced when the calculated values are decreased.

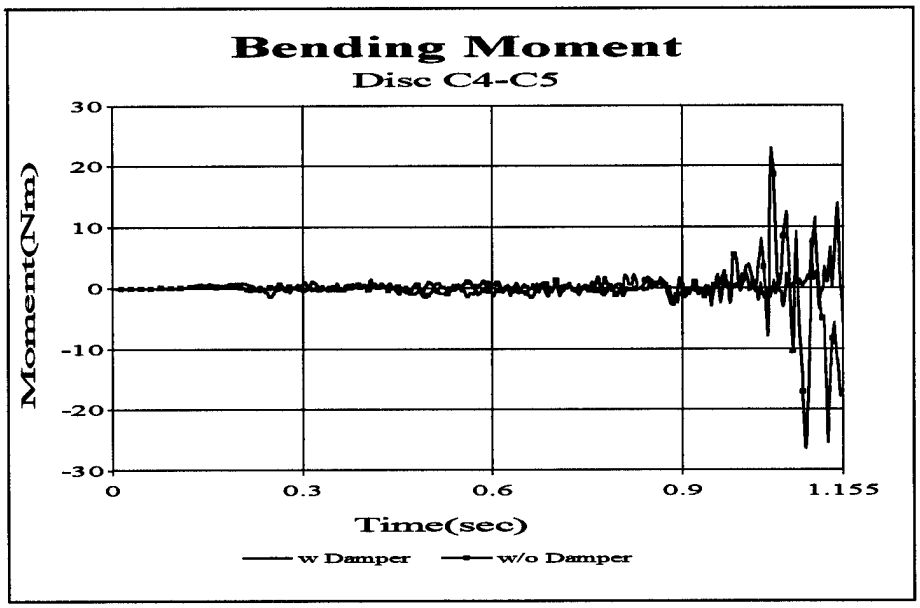

Figure 48. Comparison of Bending Moments at the Disc between C4 and C5

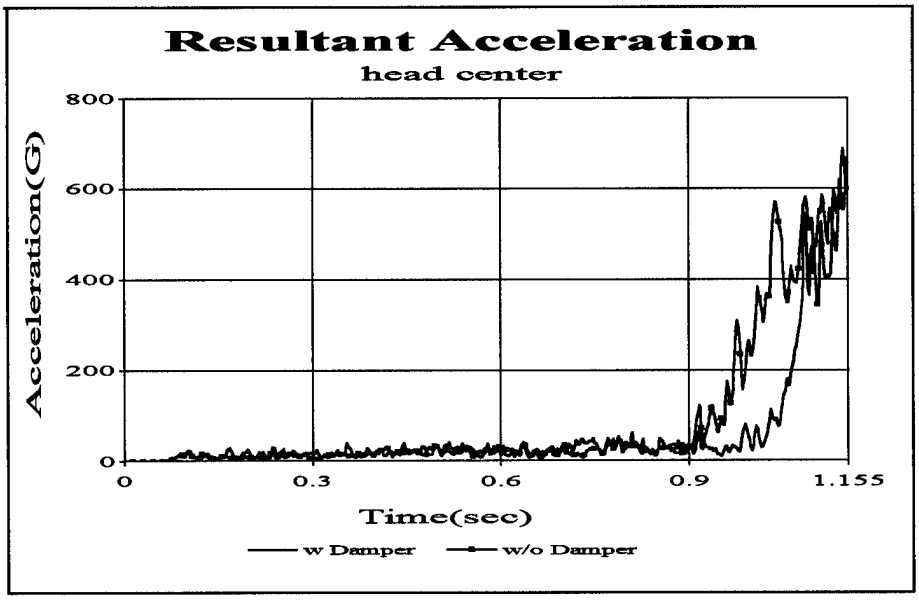

Figure 49. Comparison of Resultant Accelerations at the Center of Head

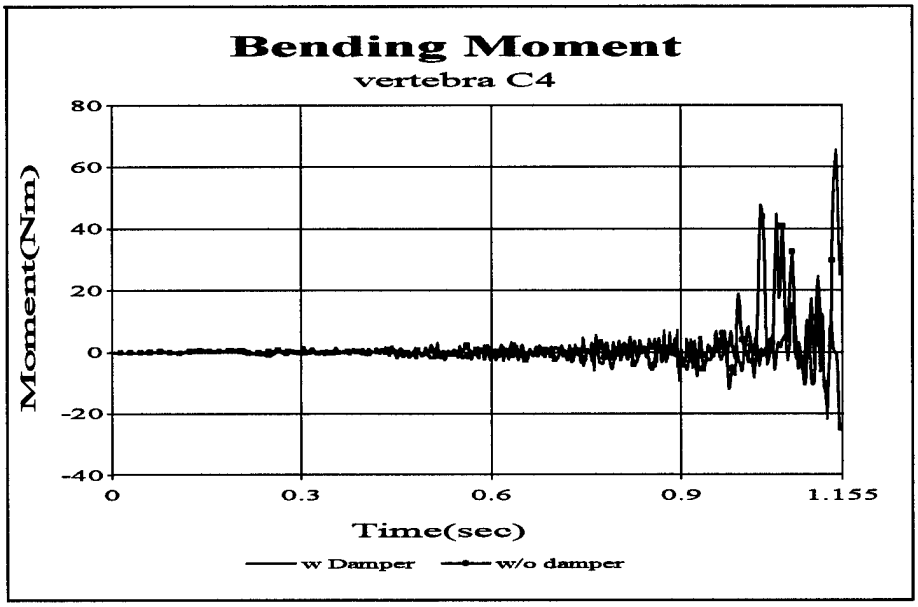

Figure 50. Comparison of Bending Moments at the Vertebra C4

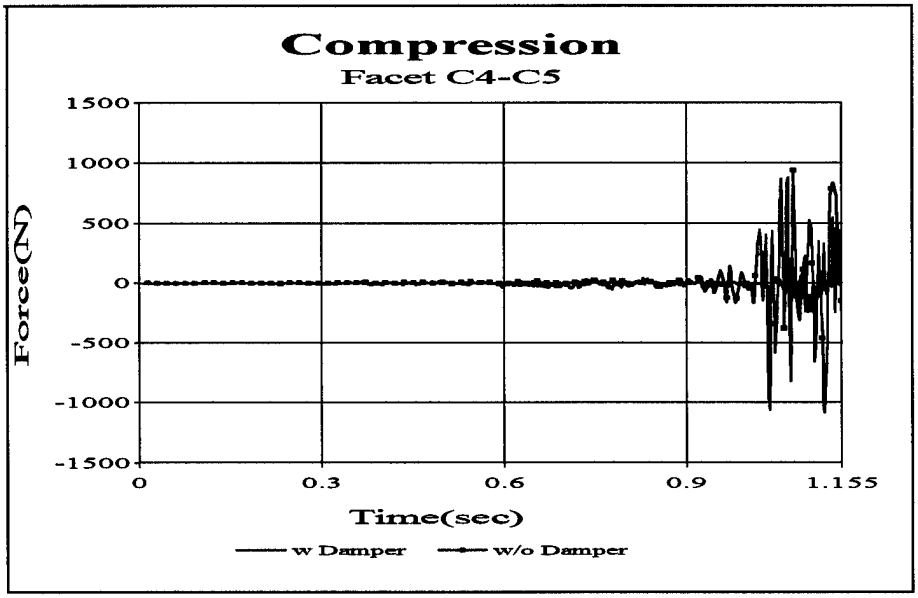

Figure 51. Comparison of Compressions at the Facet Joint between C4 and C5

Table 10. Summary of the Results

Body Part	Load	Original Model	Modified Model	Tolerance Value
Brain	HIC	9600	6040	1000
Disc	Bending	23.03	13.88	11 N-m
	Compression	5780	1694	74 N
	Torsion	9.473	6.067	1.8 N-m
Vertebra	Bending	67	24.66	19.6 N-m
	Compression	2585	2525	3620 N
Facet	Compression	1479	657.6	1720 N
Ligament	Tension	0.4 e-03	0.15e-03	76 N
Femur	Compression	1636	1640	5156 N

VI. CONCLUSIONS AND RECOMMENDATIONS

A. CONLUSIONS

The injury tolerance levels used in this study were chosen with conservative perspective from the literature survey. A small variation between estimated values and tolerance values were negligible because of the wide range variation in the material properties of the human body. Results of the previous chapters provide conclusions of this study as:

1. Life-threatening severe brain injury was expected for both models. The application of the damper for the original model reduced the HIC value up to 25%. In order to reduce brain injury potential, further modifications of the original model are required.

2. The injury in the vertebral disc of the cervical spine was caused in both models by the axial compression and torsional moment. The disc dislocation by the shear load unlikely happened for both models. The modified model reduced the possibility of disk failure caused by bending moment.

3. The vertebrae were considered safe under the axial compression. The modified model provided an element of safety to the vertebral injury caused by the bending. The calculated bending moment was decreased by almost 60% by adding dampers.

4. Facet dislocation or fracture might not occur for both models. However, the result of the original model could be interpreted as the potential injury.

5. The possibility of the injury to the femur for both models was very low. The evaluation values from both models were far below the tolerance value.

B. RECOMMENDATIONS

Even if the modified model didn't provide enough safety against the PMN AP mine explosion, the modification of its original model reduced a great deal of the injury potential to the brain and neck. Further modification of the vehicle associated with seatbelts and dampers attached to the legs of a seat will provide improved safety to the

crew of military vehicles. The response of the human body seemed to be very sensitive to the location of the seatbelt, and the way it was attached body.

In conducting this research, many problems arose in order to model a human body associated with its material and mechanical properties. Using reasonable input properties associated with the human body is one of the important conditions for the successful calculation. Much research has been conducted with human cadavers or animals investigating the material properties of the human body. These researches have provided good reference values for the material properties of the human body, but research for the mechanical properties of the human skeleton structure have been minimal. For example, the rotational and translational stiffness of the facet joints were not available. Additional extensive experimental tests need to be conducted to obtain the human body properties, including tolerance values.

A simplified skeleton of the human body was used for this research. This model must be refined for improvement of the simulation. Furthermore, a life fire testing using the human cadavers would validate and improve the present modeling and simulation technique.

LIST OF REFERENCE

1. *Clinical Dictionary in Korean,* Academy Press, Seoul, Korea, 1987.

2. Albert, Damon, et. Al., *The Human Body in Equipment Design*, Havard University Press, Cambridge, Massachusetts, 1966.

3. Calais-Germain,B., *Anatomy of Movement,* Eastland Press, Seattle, WA, 1993.

4. Augustus, A. and Manohar, M., *Clinical Biomechanics of the Spine*, second edition, Lippincott-Raven Publishers, NewYork, Philadelphia, 1990.

5. *Encarta Encyclopedia,* Microsoft, CD ROM, 1998.

6. Stanley, H., et. al., *Biomechanics of Impact Injury and Injury Tolerances of the Extremities*, Society of Automotive Engineers, Inc., Warrendale, PA, 1996.

7. Crandall, J.R., et. al., "Biomechanical Response and Physical Properties of the Leg, Foot, and Ankle" in *The 40th Stapp Car Crash Conference Proceedings*, 1996, pp. 173-192, Society of Automotive Engineers, Warrendale, PA, 1996.

8. Steven Goldstein, et. al, "Biomechanics of Bone" in A. M. Nahum and J. W. Melvin, eds., *Accidental Injury: Biomechanics and Prevention*, Springer, New York, NY, 1993.

9. John W. Melvin, et. al, "Brain Injury Mechanics" in A. M. Nahum and J. W. Melvin, eds., *Accidental Injury: Biomechanics and Prevention*, Springer, New York, NY, 1993.

10. McElhaney, J.H. and B.S. Myers, "Biomechanical Aspects of Cervical Trauma" in A. M. Nahum and J. W. Melvin, eds., *Accidental Injury: Biomechanics and Prevention*, Springer, New York, NY, 1993.

11. Robert Levine, "Injury to the Extremities" in A. M. Nahum and J. W. Melvin, eds., *Accidental Injury : Biomechanics and Prevention*, Springer, New York, NY, 1993.

12. Oglesby, D.B., *Human Male and Female Biodynamic Response to Underwater Explosion Events,* Thesis, Naval Postgraduate School, Monterey, CA, March 1998.

13. Moisey, B. and Dilip, B., "LS-DYNA3D Finite Element Model of Side Impact Dummy SID" in the *Proceedings of the Tenth International Conference on Vehicle Structural Mechanics and CAE* , pp. 107-116, Society of Automotive Engineers, Warrendale, PA, 1997.

14. *Anthropomorphic Dummies for Crash and Escape System Testing*, AGARD Advisory Report 330, 1996.

15. Gilbert, F. and Kenneth, J., Explosive Shocks in Air, 2nd edition, Springer- Verlag New York Inc, 1985.

16. King, Q.M., Investigation of Biomechanical Response due to Fregment Impact on Ballistic Projective Helmet, Thesis, pp 19-22, Naval Postgradute School, Monterey, CA, March 1998.

17. *LS-DYNA manual*, Version 940, Livermore Software Technology Corporation, Livermore, CA, 1997.

18. Stekes, J.D., et. al., *The Abbreviated Injury Scale 1980 Revision*, American Association for Automotive Medicine, Morton Grove, IL, 1980.

19. Mertz, H. J., " Anthromorphic Test Devices" in A. M. Nahum and J. W. Melvin, eds., *Accidental Injury : Biomechanics and Prevention*, Springer, New York, NY, 1993.

20. Belytschko.T, et. al.,Refinement and Validation of a Three Dimensional Head-Spine Model, University of Illinois at Chicago, Chicago, Illinois, Aug. 1978.

INITIAL DISTRIBUTION LIST

No. Copies

1. Defense Technical Information Center 2
   8725 John J. Kingman Rd., STE 0944
   Ft. Belvoir, VA 22060-6218

2. Dudley Knox Library 2
   Naval Postgraduate School
   411 Dyer Rd.
   Monterey, CA 93943-5101

3. Professor Young W. Kwon, Code ME/Kw 2
   Department of Mechanical Engineering
   Naval Postgraduate School
   Monterey, CA 93943

4. Professor Y.S. Shin, Code ME/Sg 1
   Department of Mechanical Engineering
   Naval Postgraduate School
   Monterey, CA 93943

5. Naval/Mechanical Engineering Curricular Office (Code34) 1
   Department of Mechanical Engineering
   Naval Postgraduate School
   Monterey, CA 93943

6. JUSMAG-K 2
   Unit #15339
   APO AP 96203-0187

7. KyuSang Lee 2
   666 Casanova Ave. APT #D
   Monterey, CA 93943